eLife

Reviewed Preprint
v2 • September 30, 2025
Revised by authors

Reviewed Preprint
v1 • January 3, 2025

Plant Biology

Companion cells with high florigen production express other small proteins and reveal a nitrogen-sensitive *FT* repressor

Hiroshi Takagi, Shogo Ito, Jae Sung Shim, Akane Kubota, Andrew K Hempton, Nayoung Lee, Takamasa Suzuki, Jared S Wong, Chansie Yang, Christine T Nolan, Kerry L Bubb, Cristina M Alexandre, Daisuke Kurihara, Yoshikatsu Sato, Yasuomi Tada, Takatoshi Kiba, Jose L Pruneda-Paz, Christine Queitsch, Josh T Cuperus, Takato Imaizumi

Department of Biology, University of Washington, Seattle, United States • Center for Gene Research, Nagoya University, Nagoya, Japan • Bioscience and Biotechnology Center, Nagoya University, Nagoya, Japan • Institute for Advanced Research (IAR), Nagoya University, Nagoya, Japan • Department of Botany, Graduate School of Science, Kyoto University, Kyoto, Japan • School of Biological Sciences and Technology, Chonnam National University, Gwangju, Republic of Korea • Division of Biological Science, Nara Institute of Science and Technology, Nara, Japan • Research Institute of Molecular Alchemy (RIMA), Gyeongsang National University, Jinju, Republic of Korea • Department of Biological Chemistry, College of Bioscience and Biotechnology, Chubu University, Kasugai, Japan • Department of Genome Sciences, University of Washington, Seattle, United States • Institute of Transformative Bio-Molecules (WPI-ITbM), Nagoya University, Nagoya, Japan • Division of Biological Science, Graduate School of Science, Nagoya University, Nagoya, Japan • Graduate School of Bioagricultural Sciences, Nagoya University, Nagoya, Japan • RIKEN Center for Sustainable Resource Science, Yokohama, Japan • School of Biological Sciences, University of California, San Diego, La Jolla, United States • Center for Circadian Biology, University of California, San Diego, La Jolla, United States • Brotman Baty Institute for Precision Medicine, University of Washington, Seattle, United States

eLife Assessment

This **fundamental** study uncovers the unique molecular features of Arabidopsis phloem companion cells that highly express FLOWERING LOCUS T (FT). These FT-expressing cells constitute a distinct subpopulation marked by elevated ATP biosynthesis and co-expression of small mobile proteins such as FLP1 and BFT, highlighting a fine balance between florigen and anti-florigen signals. Motif analyses and transgenic studies further identify NIGT1 transcription factors as direct, nitrogen-inducible repressors of FT, providing a mechanism for delayed flowering under nitrogen-rich conditions. Together, the **compelling** findings show that florigen-producing companion cells integrate energy metabolism, systemic protein signals, and nutrient-responsive repression to fine-tune the seasonal and nutritional regulation of flowering.

https://doi.org/10.7554/eLife.102529.2.sa3

Abstract

The precise onset of flowering is crucial to ensure successful plant reproduction. The gene *FLOWERING LOCUS T* (*FT*) encodes florigen, a mobile signal produced in leaves that initiates flowering at the shoot apical meristem. In response to seasonal changes, *FT* is induced in phloem companion cells located in distal leaf regions. Thus far, a detailed molecular characterization of the *FT*-expressing cells has been lacking. Here, we used bulk nuclei RNA-seq and single nuclei RNA (snRNA)-seq to investigate gene expression in *FT*-expressing cells and other phloem companion cells. Our bulk nuclei RNA-seq demonstrated that *FT*-expressing cells in cotyledons and true leaves showed differences especially in *FT* repressor genes. Within the true leaves, our snRNA-seq analysis revealed that companion cells with high *FT* expression form a unique cluster in which many genes involved in ATP biosynthesis are highly upregulated. The cluster also expresses other genes encoding small proteins, including the flowering and stem growth inducer FPF1-LIKE PROTEIN 1 (FLP1) and the anti-florigen BROTHER OF FT AND TFL1 (BFT). In addition, we found that the promoters of *FT* and the genes co-expressed with *FT* in the cluster were enriched for the consensus binding motifs of NITRATE-INDUCIBLE GARP-TYPE TRANSCRIPTIONAL REPRESSOR 1 (NIGT1). Overexpression of the paralogous *NIGT1.2* and *NIGT1.4* repressed *FT* expression and significantly delayed flowering under nitrogen-rich conditions, consistent with NIGT1s acting as nitrogen-dependent *FT* repressors. Taken together, our results demonstrate that major *FT*-expressing cells show a distinct expression profile that suggests that these cells may produce multiple systemic signals to regulate plant growth and development.

Introduction

Plants determine the seasonal timing of flowering based on environmental cues such as day length and temperature (1–6). The small protein FLOWERING LOCUS T (FT) is a florigen, a mobile signaling molecule that promotes flowering (7–10). In *Arabidopsis thaliana*, some phloem companion cells residing in the distal parts of leaves highly express *FT* (11, 12). Although *FT* exhibits only a single expression peak in the evening under common laboratory long-day (LD) conditions, *FT* is highly expressed in the morning and evening under natural light conditions (13, 14). The discrepancy between natural and laboratory conditions can be attributed to differences in the red-to-far-red light (R/FR) ratios. Adjusting the R/FR ratio to that observed in nature is sufficient to recreate the bimodal expression pattern of *FT* in the lab (13, 14).

Despite extensive research on the genetic regulation of *FT* expression and function, our understanding of the cells that express *FT* is limited (6). Although *FT* is expressed in some phloem companion cells, the precise molecular features that distinguish *FT*-expressing phloem companion cells from other companion cells have remained elusive (6). Recently, to understand the distinct features of *FT*-expressing cells, we employed Translating Ribosome Affinity Purification (TRAP)-seq, a method that identifies ribosome-associated transcripts in specific tissues or cell types (15). We found that the list of differentially translated transcripts in *FT*-expressing cells partially overlapped with that in the general phloem companion cell marker gene *SUC2*-expressing cells but also contained unique transcripts to *FT*-expressing cells (15). This supports the notion that the *FT*-expressing cells are similar but different from general phloem companion cells (11, 12). Our TRAP-seq datasets showed that several *FT* positive and negative transcriptional regulators and proteins involved in FT protein transport were specifically enriched in *FT*-expressing cells. We also found that a gene encoding the small protein FPF1-LIKE PROTEIN 1 (FLP1) is highly expressed in *FT*-expressing cells under LD conditions with adjusted R/FR ratio (hereafter, LD+FR conditions), but not under standard laboratory LD conditions (15). Further

analysis revealed that FLP1 promotes flowering and initial inflorescence stem growth, suggesting that it orchestrates flowering and inflorescence stem growth during the transition from the vegetative to the reproductive stage.

Although our bulk tissue/cell-specific TRAP-seq analysis revealed some unique characteristics of *FT*-expressing cells, we still do not know their characteristics in a single-cell resolution. As *FT* is expressed at specific times of the day in relatively small numbers of phloem companion cells, we needed a method to collect the information from these rare *FT*-expressing cells in a time-dependent manner. Single-cell RNA-seq (scRNA-seq) is a powerful tool to study different cell populations within the complexity of biological tissues. In plant studies, especially for root tissues, the most popular procedure involves protoplasting of cells and the application of Drop-seq in the 10X genomics pipeline. However, protoplasting is not ideal for isolating highly embedded phloem companion cells efficiently (16). On top of this problem, our target is *FT*-expressing companion cells at the specific time point of the *FT* morning peak, thus the time required for tissue isolation must be short, so that the isolated cells still restore the time-of-day information. To overcome these technical challenges, we deployed single-nucleus RNA-seq (snRNA-seq) combined with fluorescence-activated nuclei sorting (FANS) to isolate GFP-labeled cell-type-specific nuclei at a specific time of the day. Here, we report the unique characteristics of *FT*-expressing cells at a single-cell level and identify new, growth condition-specific transcriptional repressors of *FT*.

Results

Bulk nuclei RNA-seq analysis finds profound expression differences in *FT*-expressing cells between cotyledons and true leaves

To investigate gene expression in the nuclei of specific cell populations, we used *Arabidopsis* transgenic lines expressing the gene encoding NTF [Nuclear Targeting Fusion protein consists of the nuclear envelope-targeting WPP domain, green fluorescent protein (GFP) and biotin ligase recognition peptide (BLRP) (17)] under the control of cell type-specific promoters (Fig. S1A). In addition to the previously generated *pFT:NTF* line (15), we generated transgenic lines with *pSUC2* to capture most phloem companion cells, *pCAB2* for mesophyll cells, and *p35S* as a non-specific control (**Fig. 1A**, Fig. S1A). Although our original intention was the utilization of the INTACT (isolation of nuclei tagged in specific cell types), the method to capture tissue-specifically biotinylated nuclei using magnetic beads (17), we instead employed FANS to isolate the respective GFP-positive nuclei (18).

Although *FT* is expressed in both cotyledons and true leaves, it was heretofore unknown whether *FT*-expressing cells in cotyledons and true leaves were equivalent to one another at the whole transcriptome level or showed tissue-specific differences in transcription. The previous histological analyses of the *Arabidopsis pFT:GUS* reporter line showed that *FT* expression in true leaves was confined to the distal part of the leaf vasculature, whereas in cotyledons, *FT* expression was observed in the broader part of the vein (11, 19), suggesting different profiles of *FT*-expressing cells in cotyledons and true leaves. To exclude possible tissue-specificity as a source of noise in our single-nucleus data, we conducted bulk nuclear RNA-seq of GFP-positive nuclei isolated from either cotyledons or true leaves. To do so, we harvested cotyledons and the first set of two true leaves from two-week-old transgenic plants grown under LD+FR conditions at Zeitgeber time 4 (ZT4), the time of the *FT* morning expression peak, and isolated GFP-positive nuclei within an hour using a cell sorter (Fig. S1A, C). We successfully collected GFP-positive nuclei from both cotyledons and true leaves for all transgenic lines (Fig. S2) and conducted bulk RNA-seq.

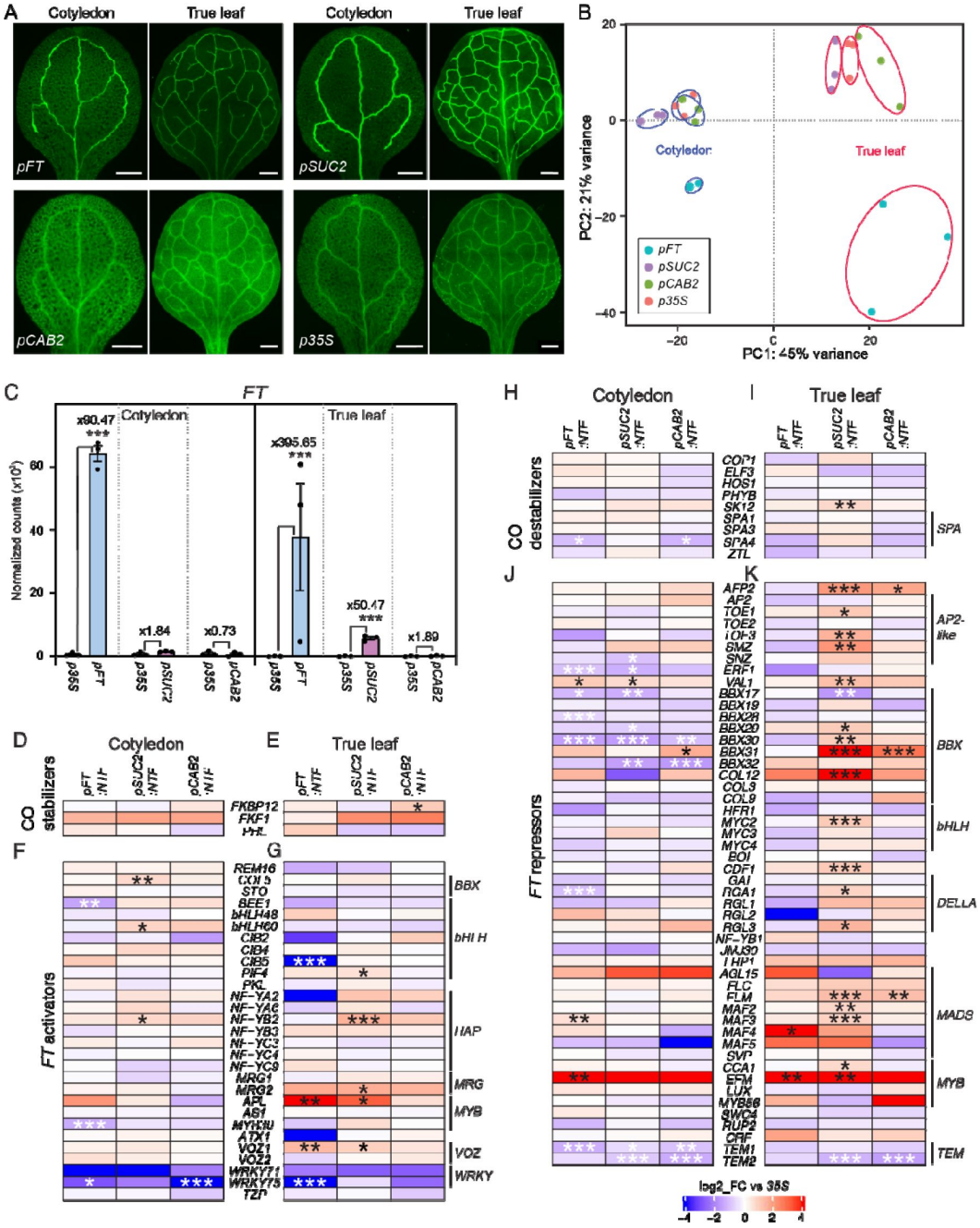

Figure 1.

Tissue-and cell-type-specific gene expression in cotyledons and true leaves.

(A) Representative images of ClearSee-treated cotyledons and true leaves of *pFT:NTF*, *pSUC2:NTF*, *pCAB2:NTF* and *p35:NTF* lines. Scale bar, 500 μm. (B) The first two principal components of bulk RNA-seq analysis for three independent cotyledon and true leaf samples. Cotyledon and true leaf samples are circled in blue and red, respectively. (C) DEseq2-normalized counts of *FT* transcripts in sorted nuclei for the *pFT:NFT*, *pSUC2:NFT,* and *pCAB2:NFT* lines compared to the *p35S:NTF* line. Fold enrichments of *FT* transcripts in each *NTF* line compared with those in *p35S:NTF* line are indicated. ****padj*<0.001. (D–K) Expression of genes encoding CO stabilizers (D and E), *FT* activators (F and G), CO destabilizers (H and I), and *FT* repressors (J and K) in cotyledons (D, F, H and J) and true leaves (E, G, I and K). Genes encoding proteins belonging to the same family were clustered in the heatmap. Bar color indicates log2-scaled fold-change relative to the *p35S:NTF* line. Asterisks denote significant differences from *p35S:NTF* (**padj*<0.05; ***padj* <0.01; ****padj* <0.001). CO was removed from the analysis due to insufficient reads at ZT4.

The principal component analysis (PCA) of the resulting expression data indicated separation by tissue and targeted cell population (**Fig. 1B**). Interestingly, the biggest difference among these datasets was the difference between cotyledons and true leaves, rather than a cell/tissue-type difference. Among different cells/tissues, *FT*-expressing cells show a distinct gene expression profile compared with other cell/tissue types examined.

Next, to ensure that we had properly enriched for the targeted cell populations, we conducted pairwise comparisons between the *p35S:NTF* control line and the cell type-specific *NTF* lines (Data S1–6). As expected, in true leaves of the *pSUC2:NTF* line, phloem companion cell marker genes *FT*, *SUC2*, *AHA3*, *APL*, *CM3,* and *AAP4* showed higher expression than in the *p35S:NTF* line, and the *pFT:NTF* line showed strong upregulation of *FT* in both cotyledon and true leaves (**Fig. 1C**, Fig. S3A–E). True leaves of the *pFT:NTF* line also showed upregulation of other phloem companion cell marker genes such as *AHA3*, *APL,* and *AAP4*; however, cotyledons of the *pFT:NTF* line only showed upregulation of *AAP4* (Fig. S3A–E), indicating some of known vascular marker genes are more suitable for representing vascular tissues in true leaves.

Similarly, in the *pSUC2:NTF* line, we observed differences in cell marker gene expression between cotyledons and true leaves. In cotyledons of the *pSUC2:NTF* line, *CM3* and *AAP4* were upregulated, but not *SUC2*, *FT*, *AHA3* and *APL*. To ensure that FANS properly enriched nuclei from *pSUC2:NTF* cotyledons, we checked the spatial expression pattern of each gene that was highly expressed in *pSUC2:NTF* cotyledons [adjusted *P*-value (*padj*) < 0.05, fold-change > 2-fold, Table S1]. The majority of the genes upregulated in the cotyledons of our *pSUC2:NTF* line were found to be expressed in the vasculature. As expected, expression of mesophyll marker gene *CAB2* was significantly lower in *pSUC2:NTF* cotyledon samples (*padj* = 1.5 x 10^{-4}), in addition to the mesophyll cell marker *RBCS1A* in true leaf samples, suggesting that a significant amount of mesophyll cells was successfully removed by FANS (Fig. S3F, G).

Having ensured proper enrichments of the targeted nuclei, we compared global changes in expression among the tested transgenic lines. Consistent with the PCA analysis, the vast majority of differentially expressed genes within a given transgenic line did not overlap between cotyledons and true leaves (Fig. S4, S5). Next, we compared the expression of known *FT* positive and negative regulators in cotyledons and true leaves of the *pFT:NTF, pSUC2:NTF,* and *pCAB2:NTF* lines (**Fig. 1D–K**) (6).

Among the transcription factors that promote *FT* expression, *APL* and *VOZ1* were upregulated in true leaves of the *pFT:NTF* and *pSUC2:NTF* lines (**Fig. 1G**). In true leaves of the *pSUC2:NTF* line, a CO destabilizing factor was significantly upregulated (**Fig. 1I**), in addition to TFs that repress *FT* expression (**Fig. 1K**). In contrast to *pSUC2:NTF* true leaves, true leaves of the *pFT:NTF* line did not show significant upregulation for most of these *FT* repressors. This lack of *FT* repression appears to be crucial for specifying *FT*-expressing cells. In contrast, there were far fewer expression differences in cotyledons between the *pFT:NTF* and *pSUC2:NTF* lines, indicating that the respective cells in true leaves have diverged more than comparable ones in cotyledons.

Similarly, *FT* expression and FT transport appeared to be more tightly associated in true leaves than in cotyledons. As reported, the expression of the FT transporter gene *FTIP1* is highly associated with *FT* expression (15). Consistent with this earlier finding, among FT transporter genes, we observed significant upregulation of *FTIP1* expression in true leaves of the *pSUC2:NTF* and the *pFT:NTF* lines but not in the respective cotyledon samples (Fig. S3H–K).

To further support true leaves as most suitable for investigating *FT*-expressing cells, we performed Terms enrichment analysis with Metascape (20). In the *pFT:NTF* line, the genes involved in the "regulation of reproductive process" were upregulated in both cotyledons and true leaves, while the genes related to the term "long-day photoperiodism, flowering" were only upregulated in the true leaf samples of the *pFT:NTF* line (Fig. S4).

snRNA-seq revealed subpopulation of phloem companion cells that highly express *FT*

Next, we used true leaves of the *pFT:NTF* and *pSUC2:NTF* lines for snRNA-seq using the 10X Genomics Chromium platform (Fig. S1B). We captured a total of 1,173 nuclei for the *pFT:NTF* line and 3,650 nuclei for the *pSUC2:NTF* line. In total, we captured 4,823 nuclei and detected 20,732 genes, a median of 149 genes per nuclei (**Fig. 2A, B**). Gene expression of these nuclei were projected in a two-dimensional UMAP as 11 different clusters (21) (**Fig. 2**). The nuclei in clusters 8 and 10 showed substantially higher number of transcripts than other clusters (Fig. S6A and B). Because this discrepancy made comparisons difficult, we focused on analyzing gene expression in the other clusters.

We first asked which nuclei highly expressed *FT*. These nuclei resided in cluster 7 (**Fig. 2D, 2E**). *SUC2* expression showed a far broader distribution across clusters than *FT* expression (**Fig. 2F**). The nuclei in cluster 7 significantly highly expressed 268 genes compared with total population (Data S7). Among these genes, we found *FLP1* (**Fig. 2G**), a gene encoding a flowering-promoting factor acting in parallel with FT (15). Next, we cross-checked these 268 genes with genes identified in the previous TRAP-seq experiment (15). 202 of the 268 genes showed higher expression in *FT*-expressing cells (*pFT:FLAG-GFP-RPL18*) than in whole companion cells (*pSUC2:FLAG-GFP-RPL18*) (Fig. S7A) in the prior study, validating our single nuclei analysis.

Further, *FKBP12*, a gene encoding a CO stabilizing protein was expressed in cluster 7 (Fig. S7B).

To explore the *FT*-expressing cluster 7, we conducted Terms enrichment analysis using Metascape (20). Genes involved in "Oxidative phosphorylation" were enriched in cluster 7 (Fig. S7C), suggesting that ATP synthesis is particularly active in nuclei belonging to this cluster (**Fig. 2H**). Genes involved in proton-generating complex I–IV and ATP synthesizing complex V in mitochondrion membrane were also upregulated in cluster 7 (Fig. S8D), suggesting that the entire ATP synthesis pathway is activated in *FT*-expressing nuclei. Additional terms such as "generation of precursor metabolite and energy" and "purine nucleotide triphosphate metabolic process," further indicated upregulation of ATP production. Since phloem companion cells actively hydrolyze ATP to generate proton gradients to load sucrose and amino acids (22), it is plausible that *FT*-expressing phloem companion cells generate a substantial amount of ATP for transport.

We next inquired about the characteristics of other phloem nuclei clusters. Like cluster 7, cluster 4 showed significantly higher *SUC2* expression compared with other clusters, suggesting companion cell identity (**Fig. 2F**, Data S7). Moreover, the genes *LTP1*, *MLP28*, and *XTH4* were upregulated in cluster 4, consistent with prior studies showing their exclusive expression in vascular tissues (particularly in the main vein) that include phloem (Fig. S8A–C) (23–25). Terms enrichment analysis found that genes encoding aquaporin were enriched in cluster 4 (**Fig. 2I**, Fig. S8D, E). To understand which part of leaf tissue consists of cluster 4 cells, we marked the promoter activity of *PLASMA MEMBRANE INTRINSIC PROTEIN 2.6* (*PIP2;6*), an aquaporin gene highly expressed in cluster 4, using the GFP-fusion protein (Fig. S8F). It showed the strongest signal in the main vein, consistent with the previous GUS reporter assay (26). Taken together, the nuclei in cluster 4 are likely to be derived from phloem cells in the main vein that are active in solute transport.

Cluster 5 is mostly composed of nuclei from the *pSUC2:NTF* line (464 out of 515 nuclei) (Fig. S6B). The nuclei in this cluster showed differentially expressed genes related to defense (Fig. S9A). Specifically, *MYC2*, a master regulator of response to jasmonic acid (JA), and the JA biosynthetic genes *LOX3*, *LOX4*, *OPR3*, and *OPCL1*, are expressed in cluster 5 (Fig. S9B). These genes are known to be expressed in vascular tissues, with *OPR3* expressed in phloem companion cells and *LOX3/4* in phloem (27–29). This subpopulation of phloem cells appears to play pivotal roles in JA-dependent defense responses. We did not include a nuclei fixation step in our FANS protocol,

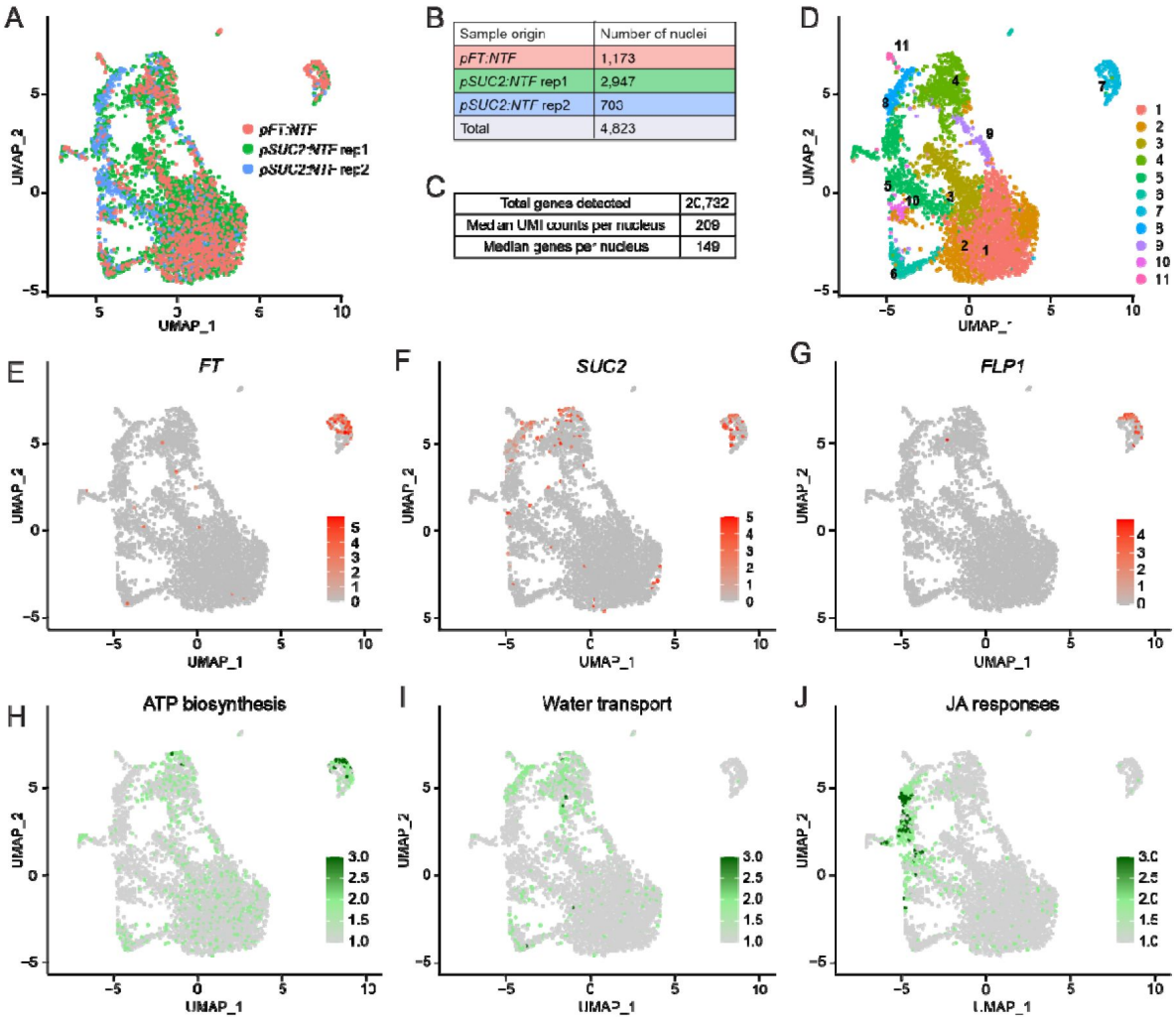

Figure 2.

Single-nucleus RNA-seq identifies distinct subpopulations of phloem companion cells.

(A) UMAP with the origin of nuclei indicated by color. (B and C) Table with the number of nuclei originated from each line and sample (B) and median UMI and number of genes detected per nucleus (C). (D) Seurat defined clusters with cluster numbers indicated. (E–G) UMAP annotated with normalized read counts for *FT* (E), *SUC2* (F), and *FLP1* (G) expression. (H–I) UMAP annotated with average read counts of genes related to ATP biosynthesis (H), water transport (I), and JA responses (J). Color bars indicate gene expression levels. For the lists of genes, see Fig. S7D (pink highlighted), S8E and S9B.

because we encountered tissue/nucleus clumping with fixation, which caused an issue in the sorting process. Because these cells were not fixed, the nuclei isolation process may have triggered wounding responses due to chopping samples before the sorting process (Fig. S1B).

Cluster 6 consisted of both phloem parenchyma and bundle sheath cells (Fig. S10A–F). Subclustering revealed that the nuclei in the upper part of cluster 6 expressed phloem parenchyma marker genes, and the nuclei in the lower part expressed bundle sheath marker genes (16) (Fig. S10C–F). Overall, the genes expressed in this cluster were enriched for genes functioning in sulfur metabolisms (Fig. S10G), including glucosinolate biosynthesis (Fig. S10H). A previous study showed that sulfur metabolic and glucosinolate biosynthetic genes are actively expressed in bundle sheath cells (30).

Lastly, Clusters 1, 2, and 3 showed expression of mesophyll cell marker genes (Fig. S6C–F), suggesting that some mesophyll cells were included during the sorting process. This result might be due to weak induction of the *FT* and *SUC2* promoters in mesophyll cells (15). Indeed, we found both genes to be expressed at low levels in mesophyll protoplasts (Fig. S11). In summary, using snRNA-seq combined with FANS, we revealed the presence of a unique subpopulation of cells with high nuclear *FT* expression. In these nuclei, genes related to ATP synthesis were enriched. Moreover, we identified other phloem cell clusters enriched for genes in water transport and JA response, which were not previously reported (16).

Next, we subclustered the nuclei in cluster 7, finding three subclusters (**Fig. 3**). Subcluster 7.2 contained the nuclei with the highest *FT* expression, in addition to expression of the companion cell marker genes, *SUC2* and *AHA3*. These nuclei contained fewer transcripts of the mesophyll marker genes *RBCS1A*, *CAB3,* and *CAB2* (**Fig. 3C, D**), consistent with a prior scRNA-seq study showing the negative correction between the expression of vasculature and mesophyll cell marker genes (31). The vascular tissue located at the distal part of true leaves, where *FT* is expressed highly, is developmentally old, whereas veins emerging from the bottom part of leaves are developmentally young (32). Thus, subcluster 7.3 may be comprised of nuclei from developmentally younger companion cells that have not fully matured yet, whereas those in subcluster 7.2 are older and have gained a stronger companion cell identity.

Phloem companion cells with high *FT* expression express other genes encoding small proteins

In LD+FR conditions, *FT*-expressing cells also express *FLP1*, which encodes another small protein with systemic effects on flowering and inflorescent stem growth (15). We asked whether the cluster 7 nuclei might express other genes encoding small proteins, which could move through phloem flow. Indeed, the median number of amino acids encoded in the differentially expressed genes of cluster 7 is smaller than those in clusters 4 and 5 (**Fig. 4A**). To validate whether high *FT*-expressing vascular cells co-express genes specifically upregulated in cluster 7, which encode small proteins, we selected eight such genes and generated their respective promoter fusions with *H2B-tdTomato* in the *pFT:NTF* background. The spatial expression patterns of these eight genes and high *FT* signals overlapped (**Fig. 4B**, S12). *FT* and cluster 7-enriched genes examined tended to express highly in the distal part of minor veins, but weakly in the main vein adjacent to the petiole, showing a clear difference from the cluster 4-enriched gene *PIP2;6* that is expressed highly in the main vein (Fig. S8F, S12). It should also be noted that the spatial expression patterns of *FT* and other cluster 7-enriched genes did not completely overlap; there were cells expressing only one of them at high levels (Fig. S12, S13).

To assess the biological significance of *FT* generated from cluster 7, we knocked down *FT* transcripts using an artificial microRNA (amiRNA) targeted to *FT* (*amiR-ft*) controlled by the promoter of cluster 7-enriched *ROXY10* gene. As a comparison, we also expressed the *amiR-ft* gene

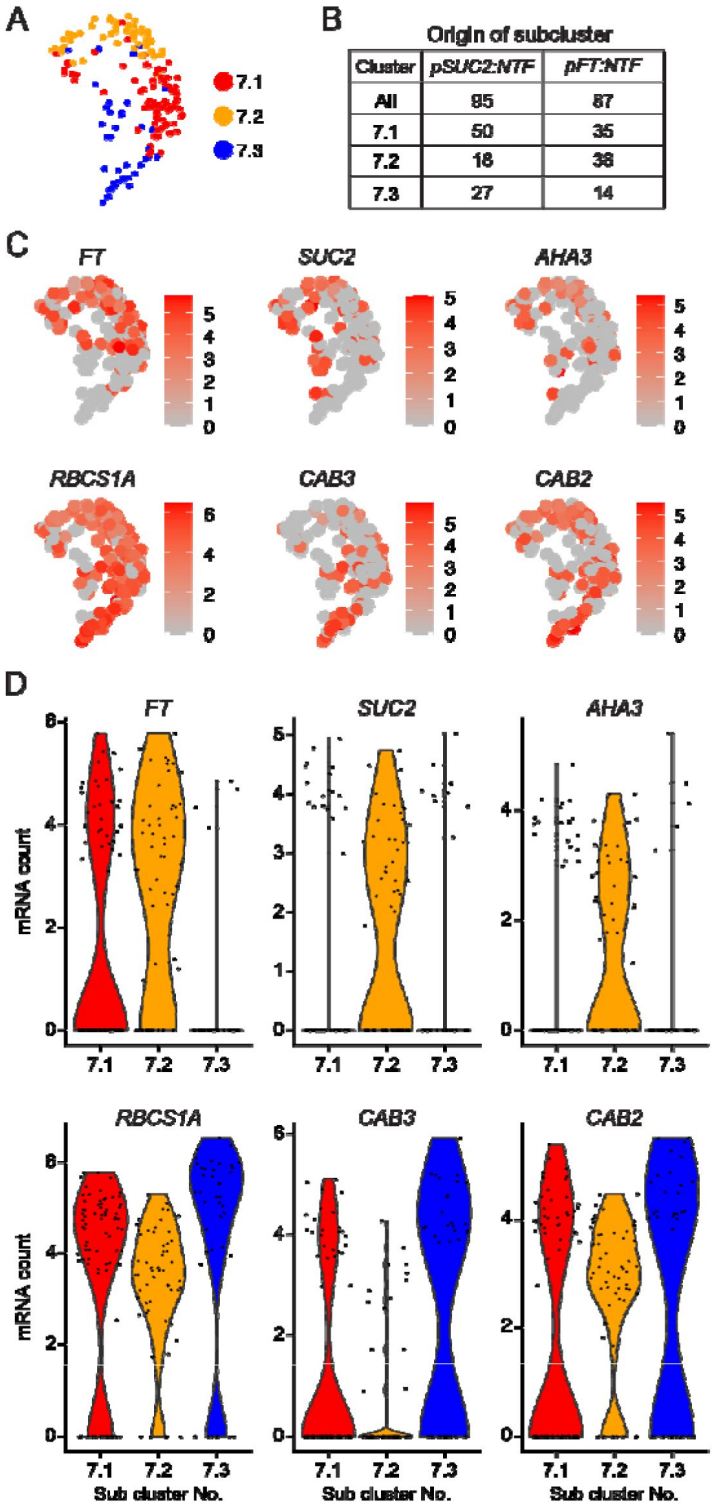

Figure 3.

Phloem companion cell and mesophyll cell marker gene expression in cluster 7.

(A) Subclustering of cluster 7. Colors indicate each subcluster. (B) Table showing the number of nuclei originated from each *NTF* line in cluster 7. (C) UMAP of normalized read counts of companion cell marker genes (*FT*, *SUC2*, and *AHA3*) and mesophyll cell marker genes (*RBCS1A*, *CAB3*, and *CAB2*). (D) Violin plot of normalized read counts of marker genes for companion cells and mesophyll cells across the three subclusters.

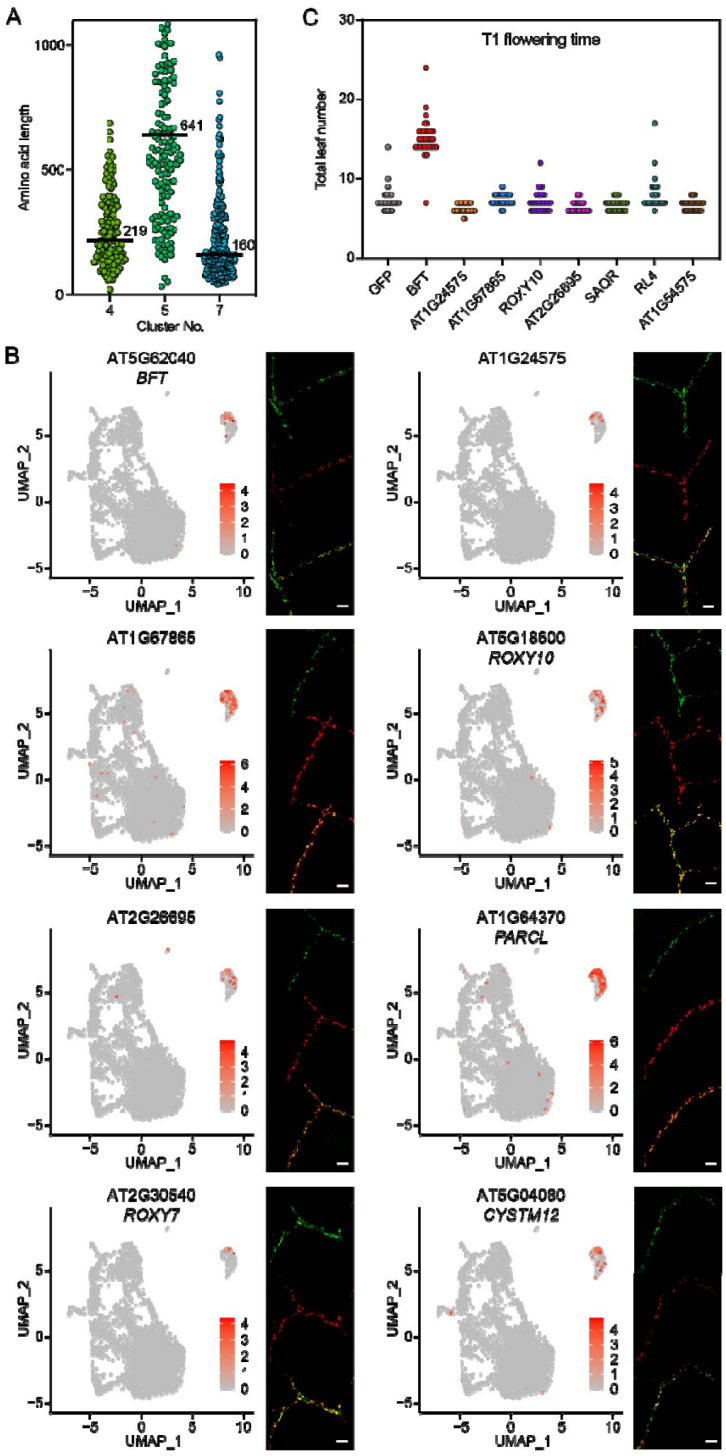

Figure 4.

FT-expressing cells express genes encoding other small proteins.

(A) Amino acid length of proteins encoded by genes differentially expressed in clusters 4, 5, and 7. Black bars indicate the median amino acid length. (B) Expression of the *pFT:NFT* line (green) and promoter fusions of selected cluster 7 genes with *H2B-tdTomato* (red) in true leaves. The selected genes were differentially expressed in cluster 7 and encoded small proteins. Yellow color shows an overlap between green and red signals. Scale bar, 50 μm. (C) Flowering time measurements of T1 transgenic plants overexpressing selected cluster 7 genes driven by the *pSUC2* promoter. Eight genes were tested, five of which were tested for overlap with *FT* expression in (B).

using *SUC2* (general companion cell-marker gene), *PIP2;6* (cluster 4-enriched gene), and *GC1* [a marker gene for guard cells where *FT* is also expressed (33)], and tested the effect on the timing of flowering at the T_1 generation. If *FT* generated from cluster 7 is important, as *ROXY10* is specifically expressed in cluster 7, late flowering of *pROXY10:amiRNA-ft* is anticipated. As a result, *pROXY10:amiRNA-ft* and *pSUC2:amiR-ft* lines severely delayed flowering (in fact, *pSUC2:amiRNA-ft* flowered later than *ft-101* mutant likely due to the effect of the hygromycin selection plate). On the other hand, *pPIP2;6:amiR-ft* was comparable with the negative control *pGC1:amiRNA-ft* line (Fig. S14A). The basal expression level of *ROXY10* was much lower than that of *SUC2* and *PIP2;6* (Fig. S14B); therefore, the delayed flowering phenotype of *pROXY10:amiR-ft* lines was not attributed to the promoter strength of genes used to drive the amiRNA. These results indicate that *FT* expressed in a relatively small but unique cluster 7 is biologically significant for flowering time regulation, although *FT* expressed in other companion cells other than cluster 7 cells may also contribute to flowering.

Next, we asked whether some of the genes enriched in cluster 7 encode new systemic flowering or growth regulators. We selected eight genes, five of which were tested for overlap with *FT* expression (**Fig. 4B**) and overexpressed each one of them using the *SUC2* promoter. Some of these genes were previously implicated in flowering. *BFT* is an *FT* homolog and acts as a floral repressor. *SENESCENCE-ASSOCIATED AND QQS-RELATED* (*SAQR*) promotes flowering under short-day (SD) conditions (34). *RAD-LIKE 4* (*RL4*) has high homology to the *RADIALIS* (*RAD*) gene in *Antirrhinum majus*, whose ectopic expression in *Arabidopsis* causes growth defects and late flowering (35). We measured the flowering time of the overexpression lines in independent T_1 plants (**Fig. 4C**). T_1 *pSUC2:BFT* plants grown under LD+FR conditions showed severely delayed flowering compared with *pSUC2:GFP* control lines (**Fig. 4C**). This result is in stark contrast to prior results obtained under standard laboratory light conditions (36), suggesting that BFT proteins might be mobile or more functionally active under natural light conditions. None of the other transgenic lines showed noticeable changes in flowering time.

Motif enrichment analysis and transgenic studies identify *NIGT1* transcription factors as direct *FT* repressors

We performed motif enrichment analysis on the promoters of the 268 genes differentially expressed in cluster 7 (37, 38), using randomly selected 3,000 genes as a control set. The most enriched motif was the motif of the NITRATE-INDUCIBLE GARP-TYPE TRANSCRIPTIONAL REPRESSOR 1.2 (also known as HHO2, $P = 9.3 \times 10^{-6}$) (**Fig. 5A**; Data S8). Although the NIGT1/HHO transcription factors (TFs) are primarily known as repressors of genes involved in nitrate uptake, constitutive expression of *NIGT1.2* significantly decreases *FT* expression (39, 40). In fact, there are two potential NIGT1 binding sites located within and adjacent to the *shadow 1* and *2* domains (*S1 and S2*) in the *FT* regulatory region (41) (Fig. S15A). These domains are highly conserved among *Brassicaceae* species and important for *FT* transcriptional regulation.

Moreover, the NIGT1 binding motifs reside in close proximity to the CO binding motif (TGTGNNATG, CO-responsive element, CORE) (41, 42), suggesting that NIGT1 binding could affect CO binding.

We performed a yeast one-hybrid (Y1H) screen of 1,957 TFs against four tandem repeats of a short *FT* promoter sequence containing the *S1* and *S2* domains and the two NIGT1 binding sites (43, 44). We found that NIGT1.1/HHO3, NIGT1.2/HHO2, NIGT1.3/HHO1, NIGT1.4/HRS1, and HHO5 specifically bind to this sequence within the *FT* regulatory region (Data S9). Next, we overexpressed five different *NIGT1/HHO* genes using the *SUC2* promoter. At T_1 generation, we observed the late flowering phenotype in the *pSUC2:NIGT1.2* and *NIGT1.4* lines, while it appeared less clear in the *pSUC2:NIGT1.1*, *NIGT1.3*, and *HHO5* (data not shown). Therefore, we generated T_3 lines of *pSUC2:NIGT1.2* and *pSUC2:NIGT1.4* and measured their flowering time.

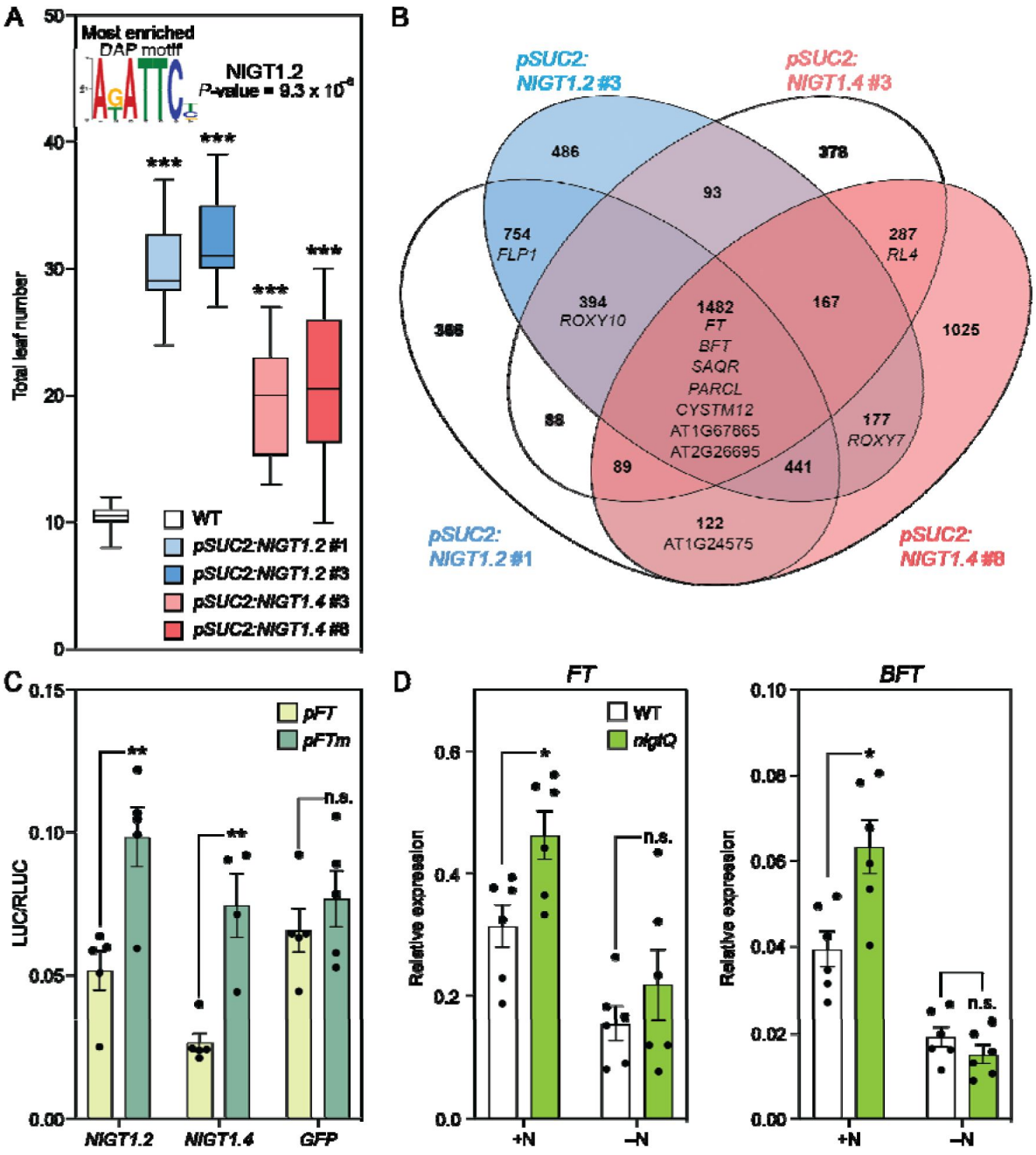

Figure 5.

NIGT1 transcription factors are repressors of *FT*.

(A) Motif enrichment analysis using the 268 genes differentially expressed in cluster 7 and flowering time of the *pSUC2:NIGT1.2* and *pSUC2:NIGT1.4* lines. The NIGT1.2 binding site was the most enriched motif in cluster 7 differentially expressed genes. The bottom and top lines of the box indicate the first and third quantiles, and the bottom and top lines of the whisker denote minimum and maximum values. The bar inside the box is the median value (n =16). (B) A Venn diagram showing the significantly down-regulated genes from bulk RNA-seq of two independent *pSUC2:NIGT1.2* and *pSUC2:NIGT1.4* lines. (C) The effect of *NIGT1.2*, *NIGT1.4* and *GFP* on wild-type and mutated *FT* promoter activity in tobacco transient assay. The 1 kb of *FT* promoter (*pFT*) and the same *FT* promoter with all NIGT1-binding sites mutated (*pFTm*) control the expression of firefly luciferase (*LUC*) gene. The LUC activity was normalized with Renilla luciferase (RLUC) activity controlled by *35S* promoter. The results are means ± SEM with each dot representing biological replicates (n = 4 or 5). (D) Relative gene expression levels of 14-day old wild-type (WT) and *nigtQ* seedlings at ZT4. Plants were grown with high nitrogen (+N) and without (–N). The results are means ± SEM with each dot representing biological replicates (n = 6). Asterisks denote significant differences from WT (*P<0.05, **P<0.01, ***P<0.001, t-test). n.s. indicates not significant.

Under LD+FR conditions, these transgenic plants flowered significantly later than wild-type plants (**Fig. 5A**). To test which genes were altered by the overexpression of *NIGT1.2* and *NIGT1.4*, we conducted RNA-seq analysis of the respective transgenic plants (**Fig. 5B**, Data. S10–13). We found that genes specifically expressed in cluster 7 such as *FT*, *BFT*, and *SAQR* were downregulated in both the *pSUC2:NIGT1.2* and *pSUC2:NIGT1.4* lines. *FLP1* expression was decreased only in *pSUC2:NIGT1.2* lines, which might explain why *pSUC2:NIGT1.2* plants exhibited a more severe late flowering phenotype than *pSUC2:NIGT1.4* plants. Similar results were obtained with qRT-PCR analysis (Fig. S16). To test if NIGT1.2 and NIGT1.4 directly regulate the *FT* promoter activity, we conducted the tobacco transient promoter luciferase (LUC) assay using the *FT* promoter (*pFT*) and the one with the mutations in three potential NIGT1 binding sites (*pFTm*) (Fig. S15B). Our data showed that co-expression of NIGT1.2 and NIGT1.4 significantly decreased the promoter activity of *pFT* compared with that of *pFTm*, while GFP did not change the *pFT* activity compared with *pFTm* (**Fig. 5C**), suggesting that NIGT1s directly repress *FT* expression level. Consistent with our snRNA-seq data (Fig. S17A, B), previous studies reported that *NIGT1.2* is expressed broadly in shoots while *NIGT1.4* is expressed only in roots (39), suggesting that *NIGT1.2* is the major player in *FT* regulation. Interestingly, neither *NIGT1.2* or *NIGT1.4* expressed highly in cluster 7. We speculate that they have a role to prevent the misexpression of *FT* and perhaps other cluster 7 genes in non-cluster 7 cells.

Ample nitrogen prolongs the vegetative growth stage and delays flowering (45); however, the detailed mechanisms of this delay remain largely unknown (45). Since *NIGT1* genes are induced under high nitrogen conditions, we tested the quadruple mutant of the *NIGT1* genes (*nigtQ* mutant) for *FT* and *BFT* expression with (+N) and without high nitrogen (–N) (39). The *nigtQ* plants showed enhanced *FT* and *BFT* expression compared to the wild-type plants under +N but not –N conditions, suggesting that the NIGT1 TFs act as novel nitrate-dependent regulators of flowering (**Fig. 5D**, S17C). To test if *nigtQ* mutations affect flowering timing under different nitrogen conditions, we transplanted 9-day-old WT and *nigtQ* seedlings grown on Murashige and Skoog-based media with 20 mM NH_4NO_3 to new media containing either 20 mM or 2 mM NH_4NO_3. The *nigtQ* plants bolted earlier in days than WT when they grew with 20 mM NH_4NO_3, whereas the flowering time of WT and *nigtQ* was almost identical under 2 mM, suggesting that *NIGT1* genes delay flowering under ample nitrogen conditions (Fig. S17D and E). However, there was no difference between WT and *nigtQ* in leaf number at bolting (Fig. S17F). Therefore, it appears that the *nigtQ* mutation enhanced overall plant growth speed rather than developmental timing of flowering. We also have counted leaf numbers of the *nigtQ* at bolting on nitrogen-rich soil. The mutant generated slightly more leaves than WT when they flowered (Fig. S17G). These results suggest that the NIGT-derived fine-tuning of *FT* regulation is conditional on higher nitrogen conditions.

Discussion

Plants utilize seasonal information to determine the onset of flowering. One of the key mechanisms of seasonal flowering is the transcriptional regulation of the florigen *FT* in leaves. Our previous study revealed that *FT*-expressing cells also produce FLP1, another small protein that may systemically promote both flowering and elongation of leaves, hypocotyls, and inflorescence stems (15). Therefore, a more detailed characterization of *FT*-expressing cells might identify additional components that are essential for the integration of the many environmental cues in natural environments into the precise timing of flowering and related developmental changes. Here, we applied bulk nuclei and snRNA-seq and transgenic analysis to examine *FT*-expressing cells at high resolution.

Differences in the spatial expression patterns of *FT* between cotyledons and true leaves are likely driven by negative regulators

In young *Arabidopsis* plants grown in LD, true leaves show *FT* expression in the distal and marginal parts of the leaf vasculature, while cotyledons express *FT* across entire veins (11, 19). We used bulk RNA-seq to examine the *FT*-expressing cells in cotyledons versus those in true leaves, using FANS-enriched nuclei. Tissue-specific differences (cotyledons vs. true leaves) in gene expression were more significant than those observed for the enriched cell populations, an unexpected result as cotyledons and true leaves are not typically treated as separate organs.

The true leaves but not the cotyledons of the *pSUC2:NTF* and *pFT:NTF* lines showed differences in the expression of *FT* negative regulators. This result suggests that *FT* expression is strongly repressed in most of the true leaf companion cells, contributing to the spatial expression pattern of *FT* observed in true leaves. In this study, we focused on the *FT* expression peak in the morning (ZT4) under LD+FR conditions; however, in the future, it would be interesting to investigate the expression patterns of *FT* regulators at the *FT* evening peak (ZT16), as our results suggest that there are two different mechanisms regulating each *FT* peak in natural long days (13, 14).

A subpopulation of phloem companion cells highly expresses *FT* and other genes encoding small proteins

Our snRNA-seq identified a cluster with nuclei derived from cells with high *FT* expression that controls flowering time. The cluster 7 nuclei are derived from cells that appear to be metabolically active and produce ATP, which may be used to upload sugars, solutes, and small proteins, including FT, into the phloem sieve elements. Based on subclustering analysis, *FT* expression levels were positively correlated with companion cell marker gene expression and negatively correlated with mesophyll cell marker gene expression. The observed shift from mesophyll to companion cell identity may represent the trajectory of companion cell development (31).

In clusters 4 and 5, we found nuclei isolated from phloem cells with high expression of aquaporin and JA-related genes, respectively. These cell populations were not identified in a previous protoplast-based scRNA-seq analysis targeting phloem (16). We speculate that these cells are highly embedded in the tissue and therefore practically difficult to isolate. Previous studies show that JA biosynthetic genes such as *LOX3/4* and *OPR3* are highly expressed in phloem including companion cells (27, 29), consistent with our results.

Aquaporin genes such as *PIP2;1* and *PIP2;6* are thought to be highly expressed in leaf xylem parenchyma and bundle sheath tissues (26). However, cluster 6, which contains nuclei isolated from bundle sheath and phloem parenchyma cells, showed fewer expressed aquaporin genes than the cluster 4 nuclei, which also expressed *SUC2*. This result might indicate that the cells active in water transport exist not only in bundle sheath or xylem parenchyma cells but also in a subpopulation of phloem cells. In summary, *SUC2*/*FT*-expressing vasculature cells consist of cell subpopulations with different functions within true leaves.

A drawback of our snRNA-seq analysis was shallow reads per nucleus. It appears mainly due to the low abundance of mRNA in FANS-isolated nuclei from 2-week-old leaves. Based on our calculation, the average mRNA level per nucleus in our isolated samples is approximately 0.2 pg (3,000 pg mRNA from 15,000 sorted nuclei). Future technological advance is needed to improve the data quality.

BFT may fine-tune the balance between flowering and growth as a systemic anti-florigen

The *FT*-expressing nuclei of cluster 7 preferentially expressed genes encoding small proteins including *FLP1*, *BFT*, and *SAQR* (34, 36, 46). Although a previous study reported that *BFT* driven by the *SUC2* promoter does not alter flowering time (36), our result shows that overexpression of this gene delays flowering under LD+FR conditions (**Fig. 4C**). This discrepancy is likely due to our use of growth conditions with the adjusted R/FR ratio that mimics natural light conditions, as the majority of our transgenic lines showed a similar late flowering phenotype.

Why do *Arabidopsis* plants produce florigen FT and anti-florigen BFT in the same cells? There is precedent for the co-expression of florigen and anti-florigen in leaves in other plants. In Chrysanthemums, a weak florigen *CsFTL1* and a strong anti-florigen *CsAFT* are both expressed in leaves in long days. Short-day conditions repress *CsAFT* but induce the expression of a strong florigen *CsFTL3* to initiate flowering (47, 48). The balance in florigen and anti-florigen expression is also important for wild tomatoes to control flowering time, and this regulation was lost in domesticated tomatoes, resulting in day-neutral flowering behaviors (49). In *Arabidopsis*, the FT-homolog floral repressor TERMINAL FLOWER 1 (TFL1) is expressed at the shoot apical meristem and competes with FT for physical interaction with FD (50). In addition to preventing precocious flowering, the presence of TFL1 is crucial for the balance between flowering initiation and stem growth because FT terminates inflorescence stem growth (51). Like FT and TFL1, BFT directly binds to FD (36), suggesting that BFT's mode of action is similar to that of TFL1. However, unlike for TFL1, loss of BFT does not affect flowering time under standard growth conditions (36, 46). The lack of a visible flowering phenotype in the *bft* knockout mutant might be due to the substantially lower expression of *BFT* compared to *FT* under standard growth conditions (36). Consistent with this interpretation, the *bft* knockout mutant is significantly delayed in flowering under high salinity conditions where *BFT* gene expression is strongly induced (36).

Thus, BFT appears to act as an anti-florigen under specific growth conditions, possibly including LD+FR conditions. Given the complexity of natural environments, the existence of multiple specialized anti-florigens might facilitate signal integration and reduce noise in the onset of flowering and stem growth.

NIGT1 TFs contribute to the nutrient-dependency of flowering time

To identify potential novel transcriptional regulators of *FT*, we identified enriched motifs in the promoters of the 268 genes that were differentially expressed in cluster 7. This analysis indicated that NIGT1 TFs may affect the expression of *FT* and other genes co-expressed with *FT*. Using Y1H screening, we found that all NIGT1s and HHO5 can bind to the enhancer sequences derived from the *FT* promoter. NIGT1s are involved in nitrogen absorption as negative regulators (39, 40). It is well-known that nitrogen availability affects the onset of flowering; however, most of the mechanistic underpinnings remain unknown. A recent study showed that ample nitrogen availability causes phosphorylation of FLOWERING BHLH 4 (FBH4), a direct positive regulator of CO, which results in attenuation of FBH4 transcriptional activity (45). This mechanism acts upstream of *FT*, whereas the NIGT1 TFs likely act as direct repressors of *FT*. Multiple nitrogen-dependent mechanisms acting on *FT* regulation might ensure the proper balance between nutrient availability and resource allocation toward developmental transitions.

Materials and Methods

Molecular cloning and plant materials

All *Arabidopsis thaliana* transgenic plants and mutants are Col-0 backgrounds. *ACT2:BirA* plant (17) was used as the *Arabidopsis* genetic background to generate *NTF* expressing lines. The *NTF* cDNA was controlled by the *35S* promoter or the tissue-specific promoters: *CAB2* (AT1G29920), *SUC2* (AT1G22710), and *FT* (AT1G65480). The *NTF* sequences were amplified using primers (5'-CACCATGGATCATTCAGCGAAAACCACACAG-3' and 5'-TCAAGATCCACCAGTATCCTCATGC-3') and cloned into the pENTR/D-TOPO vector (Invitrogen). The *CAB2* promoter region (324 bp) was amplified by the primers (5'-CACCATATTAATGTTTCGATCATCAGAATC-3' and 5'-TTCGATAGTGTTGGATTATATAGGG-3') and cloned into the pENTR 5'-TOPO (Invitrogen) (52). The *SUC2* promoter region (2,302 bp) was amplified by primers (5'-GGTGCATAATGATGGAACAAAGCAC-3' and 5'-ATTTGACAAACCAAGAAAGTAAG-3') and cloned into the pENTR 5'-TOPO. The *CAB2* and *SUC2* promoter sequences were fused with *NTF* in the binary GATEWAY vector R4pGWB501 through LR clonase reaction (53). The *CAB2:NTF* and *SUC2:NTF* constructs were transformed into wild-type Col-0. The *pFT:NTF* line was described in the previous study (15).

The *H2B-tdTomato* constructs containing promoter regions of cluster 7 highly expressed genes were made by swapping the heat-shock promoter (*pHS*) of *pPZP211 HS:H2B-tdTomato* (15). Promoter sequences were amplified by the forward primer containing SbfI site and reverse primer containing SalI site, and inserted into these restriction enzyme sites. Following primer sequences were used to amplify 2,396 bp upstream of *BFT* (AT5G62040), 5'-CCTGCAGGGACAGAGTAAATTCAACCACAGCAGGT-3' and 5'-GTCGACTTTTCTTTGCTCCAATGTGTTTGCGTTTG-3'; 2,521 bp upstream of AT1G24575, 5'-CCTGCAGGCTCTCAGATCACCGTAAGGGCATAATTATATTTAGGTTCAC-3' and 5'-GTCGACGTGATGAGATTTGTGACTGGAGGAGTTTCCAAGTACCATTCTT-3'; 2,488 bp upstream of AT1G67865, 5'-CCTGCAGGACTTCACATTCTTGGATTCCGTTTGTAATAACTAATGTTTT-3' and 5'-GTCGACCCCTCCGGCAACCCCAATAATAAGCTTATCAAGCATTTTTCTT-3'; 1,939 bp upstream of *ROXY10* (AT5G18600), 5'-CCTGCAGGGCAATGGACCGTACGTCTAGGTCACGCATCTTATCCGACAT-3' and 5'-GTCGACCACCGGTCTCTCCATCACCATCTTCGTTATCATATCCATTGCT-3'; 2,226 bp upstream of AT2G26695, 5'-CCTGCAGGAATGTAATGTATAATGTGTTCATAAACAGCACCAACTACCC-3' and 5'-GTCGACTGCGTGCTGACACGCACCACATAGCCAATCTCCTCCGGTCCAG-3'; 1,911 bp upstream of *PARCL* (AT1G64370), 5'-CCTGCAGGGCCCATCTAATTCCCATTTTAGATGCATGAGTTCAACGCTA-3' and 5'-GTCGACGCCTTGAGCCACCTCGTAGTAGTCTTTCTCACGGTTTTCGTAG-3'; 2,719 bp upstream of *ROXY7* (AT2G30540), 5'-CCTGCAGGATCACCGGTAAGTGACAAGAGAATTGA-3' and 5'-GTCGACGGTTTCTTGAAGGAGGTCTCGATCAATCT-3'; 2,574 bp upstream of *CYSTM12* (AT5G04080),5'-CCTGCAGGGAGAATTTGAAGGAGGCTTTGCGTTTTATCTGCTCATCTAA-3' and 5'-GTCGACTTGTGGAGGATTTTGATCTCTCATGTCCTGCATCTTCTCAAAA-3'. These constructs were transformed into the *pFT:NTF* plants.

To overexpress cluster 7 highly expressed genes, we amplified coding sequences using the following primer sets. *BFT*, 5'-CACCATGTCAAGAGAAATAGAGCCAC-3' and 5'-AGTTAATAAGAAGGACGTCGTCG-3'; AT1G24575, 5'-CACCATGGTACTTGGAAACTCCTCCAGTCAC-3' and 5'-GACTAGGCGCTCTTAGTCATCCAC-3'; AT1G67865, 5'-CACCATGCTTGATAAGCTTATTATTGGGGTTGCC-3' and 5'-CTTTACTCCCTGTCTTTCTGGCG-3'; *ROXY10*, 5'-CACCATGGATATGATAACGAAGATGGTGATGGAG-3' and 5'-AGTCAAACCCACAATGCACCAG-3'; AT2G26695, 5'-CACCATGAGCTGGACCGGAGGAG-3' and 5'-ATTTAGACGCCACCATAATCTCTTG-3', *SAQR* (AT1G64360), 5'-CACCATGTCGTTTAGAAAAGTAGAGAAGAAACC-3' and 5'-GATTAGTAATTAGGGAAGTGTTTGCGGC-3'; *RL4* (AT2G18328), 5'-CACCATGGCTTCTAGTTCAATGAGCACC-3' and 5'-CTTCAATTAGTGTTACGGTACCTAGG-3'; AT1G54575, 5'-CACCATGGTGGATCATCATCTCAAAGC-3' and 5'-AATTAATTATTCTTTTGTGGCTTGG-3'. Amplified

cDNA was cloned into pENTR/D-topo, followed by GATEWAY cloning using pH7SUC2, a binary vector carrying 0.9 kb *SUC2* promoter (15). These vectors were transformed into wild-type plants possessing *pFT:GUS* reporter gene (11).

For gene expression measurements and confocal imaging, surface sterilized seeds were sawn on the 1x Linsmaier and Skoog (LS) media plates without sucrose containing 0.8% (w/v) agar and stratified for more than 2 days at 4 °C before being transferred to the incubator. Plants were grown under LD+FR conditions (100 µmol photons m^{-2} s^{-1}, red/far-red ratio = 1.0) for two weeks as described previously (6). For gene expression analysis under –N conditions, plants were grown on normal 1x Murashige and Skoog (MS) medium plates with full nitrogen (+N) for 10 days and transplanted to +N and –N medium plates and grown for 4 additional days. The ion equilibrium of the medium between +N and –N was ensured by replacing KNO_3 (18.79 mM) and NH_4NO_3 (20.61 mM) by KCl (18.79 mM) and NaCl (20.61 mM). For flowering time measurements using T_1 transgenic lines (**Fig. 4B**), T_1 plants were grown on hygromycin selection plates for 10 days and transferred to Sunshine Mix 4 soils (Sun Gro Horticulture). Soils were supplemented with a slow-release fertilizer (Osmocote 14-14-14, Scotts Miracle-Gro) and a pesticide (Bonide, Systemic Granules) and filled in standard flats with inserts (STF-1020-OPEN and STI-0804, T.O. Plastics). For the same experiment using *pSUC2:NIGT1* T_3 plants (**Fig. 5B**), surface sterilized seeds were directly sawn on soils and kept in 4 °C for at least 2 days. Plants on soils were kept grown under LD+FR conditions as described previously (6). Tissue clearing and confocal imaging were conducted as previously described (6).

Nuclei isolation by FANS

Nuclei labeled with NTF proteins were isolated with the modified method described by Galbraith *et al.* (54). Cotyledons and true leaves were detached from 2-week-old plants grown under LD+FR conditions at ZT4 (approximately 100–200 seedlings were used at each sample), and placed on a mixture of 2 mL filter sterilized chopping buffer (20 mM MOPS, 30 mM sodium citrate and 45 mM $MgCl_2$) and 20 µL SUPERase-In RNase inhibitor (20 U /µL) (Thermo Fisher Scientific) (Fig. S1B and C). We did not use fixing reagents such as formaldehyde in the chopping buffer because it caused clumps of nuclei. Leaves were chopped with the razor blade in 4 °C room until finely crushed in the buffer solution, followed by the addition of 3 mL more chopping buffer and filtration with 30-µm CellTrics filter (Sysmex CORP.). It usually takes approximately 30 min from start chopping leaves to applying the samples for sorting. The filtrated sample solution was directly applied to the sorting with SH800S Cell Sorter equipped with a 100-µm flow tip (SONY). As a sheath solution, we used 0.9% NaCl but not PBS to prevent calcium precipitation by phosphate contained in PBS, which severely decreases the integrity of nuclei. DEPC-treated water was used for all buffers and solutions in this experiment to prevent RNA degradation.

Nuclei were excited by 488 nm collinear laser, and FITC and mCherry channels were used to detect GFP signal and autofluorescence, respectively. The area of GFP-positive nuclei was determined using the parental line *pACT2:BirA* (Fig. S2).

SMART-seq2 library preparation and analysis

For bulked nuclei RNA-seq, approximately 15,000 nuclei were collected from cotyledons and true leaves of *p35S:NTF*, *pCAB2:NTF*, and *SUC2:NTF* lines, while 10,000 (cotyledons) and 3,000 (true leaves) nuclei were collected from *pFT:NTF* due to fewer population of GFP-positive nuclei. Sorted nuclei were directly collected into Buffer RTL (Qiagen), and RNA was extracted according to the manufacture protocol of RNeasy Micro Kit (Qiagen). Three independent biological replicates were produced for cotyledon and true leaf of all transgenic lines.

After RNA integrity was confirmed using High Sensitivity RNA Screen Tape (Agilent), SMART-seq2 libraries were generated according to the manufacturer's protocol (Clontech). Sequencing was performed on the Illumina NovaSeq 6000 platform through a private sequencing service

(Novogene). Since reverse reads were undesirably trimmed due to the presence of in-line indexes in SMART-seq libraries, we used only forward reads of paired-end reads. Approximately 10.8 to 34.6 million forward reads (average, 20.2 million reads) were produced from each sample. By STAR software (version 2.7.6a) (55), reads were mapped to *Arabidopsis* genome sequences from The Arabidopsis Information Resource (TAIR, version 10) (*http://www.arabidopsis.org/*). DEGs were selected based on the adjusted *P*-value calculated using DEseq2 in the R environment.

Single-nucleus RNA-seq library preparation

For snRNA-seq experiments, sorted nuclei from true leaves were collected in the mixture of 100 µL 1x PBS and 10 µL SUPERase-In RNase inhibitor in a 15 mL corning tube. Prior to nuclei collection, the corning tube was coated by rotating with 10 mL 1x PBS containing 1% BSA at room temperature to prevent static electricity in the wall. After more than 10,000 nuclei were collected in the corning tube (sorting approximately for 1 hour), 10 µL of 1 mg/mL DAPI solution and 1/100 volume of 20 mg/mL glycogen (Thermo Scientific) were added and centrifugated in 1,000xg for 15 min at 4 °C. Nuclei numbers were determined using a hemocytometer after resuspension with a small volume of 1x PBS. The total number of nuclei varied depending on the plant line and trial but was no more than 11,000.

snRNA-seq was performed using the 10x Single-cell RNA-Seq platform, the Chromium Single Cell Gene Expression Solution (10x Genomics). Two biological replicates of *SUC2:NTF* and one replicate of *pFT:NTF* were produced for a total of three samples.

Estimating gene expression in individual nucleus

Sequencing of snRNA-seq reads was performed on the Illumina Nextseq 550 platform, followed by the mapping to the TAIR10 Arabidopsis genome using Cellranger version 3.0.1 software.

The Seurat R package (version 4.0.5) (56, 57) was used for the dimensional reduction of our SnRNA-seq data. To remove potential doublets and background, we first filtered out nuclei with less than 100 and more than 5,500 detected genes, and more than 20,000 UMI reads. For UMAP data visualization and cell clustering, all biological replicates were combined, and twenty principal components were compressed using a resolution value of 0.5.

Significantly highly expressed genes in each cluster compared with entire nuclei population were identified using FindMarkers in Seurat with default parameters.

To show the enrichments of specific sets of genes, average expression of ATP biosynthesis, JA responsive, aquaporin, bundle sheath and phloem parenchyma marker genes were visualized using AddModuleScore in Seurat. For bundle sheath and phloem parenchyma markers, we leveraged the top 50 most highly expressed genes in these cell types in previous protoplast-based ScRNA-seq data (16).

Protein amino acid length

Amino acid length of proteins encoded by genes highly expressed in clusters 4, 5, and 7 were obtained from the Bulk Data Retrieval tool in TAIR database (*https://www.arabidopsis.org/tools/bulk/sequences/index.jsp*).

Promoter *cis*-enrichment analysis

To identify highly enriched *cis*-elements in cluster 7 highly expressed genes, promoter sequences of 268 genes highly expressed in cluster 7 and randomly selected 3,000 genes by R coding were extracted using the Eukaryotic Promoter Database (37, 38). Obtained promoter sequences

were next submitted to Simple Enrichment Analysis (SEA) (58) in MEME Suite server (version 5.4.1) to elucidate what *cis*-elements are enriched in cluster 7 highly expressed genes through a comparison with random 3,000 genes.

Yeast one-hybrid screening

Four tandem repeats of S1/S2 elements of *FT* promoter that include a CO-responsive (CORE) element (41, 42) were generated through restriction enzyme-mediated ligation. Forward and reverse oligonucleotides containing S1/S2 element with HindIII (CORE-F1: 5'-AGCTTACTGTGTGATGTACGTAGAATCAGTTTTAGATTCTAGTA CTGTGTGATGTACGTAGAATCAGTTTTAGATTCTAG-3'), EcoRI (CORE-R1: 5'-AATTCCTAGAATCTAAAACTGATTCTACGTACATCACACAGTACTAGAATCTAAAACTGATTCT ACGTACATCACACAGTA-3'), SacI (CORE-F2: 5'-CACTGTGTGATGTACGTAGAATCAGTTTTAGATTCTAGTACTGTGTGATGTAC GTAGAATCAGTTTTAGATTCTAGGGTAC-3'), and KpnI (CORE-R2: 5'-CCTAGAATCTAAAACTGATTCTACGTACATCACACAGTACTAGAATCTAAAACTGATTCTACG

TACATCACACAGTGAGCT-3') recognition sequences were chemically synthesized from Genewiz (*https://www.genewiz.com/*). The oligonucleotides complementary to each other were denatured for 10 min at 95 LC, then annealed for 30 min at RT. The resultant product was inserted into pENTR/D-TOPO vector harboring MCS sites (HindIII, EcoRI, SacI and KpnI) through restriction enzyme-mediated ligation. Four tandem S1/S2 elements in pENTR/D-TOPO were then inserted into pY1-gLUC59-GW vector (43) using LR clonase II (Invitrogen). The resultant pY1-gLUC59-GW-2XCORE plasmids were used for Y1H screening analysis.

qRT-PCR analysis using total RNA

Total RNA extraction, cDNA synthesis and qRT-PCR were performed as previously described (6).

ISOPENTENYL PYROPHOSPHATE / DIMETHYLALLYL PYROPHOSPHATE ISOMERASE (*IPP2*) and *PROTEIN PHOSPHATASE 2A SUBUNIT A3* (*PP2AA3*) were used as reference genes. For statistical tests, relative expression levels were $\log_2$-transformed to meet the requirements for homogeneity of variance. qPCR primers used in this study are listed in Table S2.

RNA-seq analysis using total RNA

Two-week-old seedlings of *pSUC2:NIGT1.2* and *NIGT1.4* grown on 1xLS media plates under LD+FR conditions were harvested at ZT4. RNA extraction and RNA-seq library preparation were conducted as described previously (15, 59). As a reference, our previous gene expression data of wild-type plants grown at the exact same conditions was compared with *pSUC2:NIGT1* lines(15).

Tobacco transient promoter LUC assay

We amplified 1 kb upstream of *FT* (*pFT*) using the primer sets, pFT-FW (5'-CACCATAATATGGCCGCTTGTTTATA-3') and pFT-RE (5'-CTTTGATCTTGAACAAACAGGTGG-3'), and cloned it into pENTR/D-topo. To mutate 2 of 3 potential NIGT1-binding sites, we synthesized the Megaprimer #1 by PCR using the forward primer pFTmut1 (5'-CAATGTGTGATGTACGTATACTCAGTTTTAGAGTATAGTACATCAATAGACAAGAAAAAG-3') and pFT-RE. Next, to mutate the rest of NIGT1-bind site, the Megaprimer #2 was synthesized using the forward primer pFTmut2 (5'-CTACCAAGTGGGAGATATAATTTGAATTAATTCCAGTGTATTAGTGTGGTG) and Megaprimer #1. Subsequently, we amplified 1 kb promoter *FT* with mutations in all 3 NIGT1-bindning sites (*pFTm*), we amplified DNA using pFT-FW and Megaprimer #2, and cloned it into pENTR/D-topo. Finally, *pFT* and *pFTm* regions were cloned into pFLASH, the binary GATEWAY vector for promotor LUC assay (60).

The promoter LUC assay in *N. benthamiana* leaf was conducted as previously described with slight modifications (61). *Agrobacterium* carrying binary vectors was cultured in LB media containing 20 μM acetosyringone and antibiotics overnight and subsequently precipitated at 4,000 rpm at room temperature for 15 min. The *Agrobacterium* pellet was resuspended using inoculation buffer (10 mM $MgCl_2$, 10 mM MES-KOH pH5.6, and 100 μM acetosyringone). After incubation for 3 hours at room temperature, OD_{600} was adjusted to 0.2 and infiltrated into the abaxial side of tobacco leaves using a 1 mL syringe. *Agrobacterium* carrying reporters (*pFT:LUC* and *pFTm:LUC*), effector (*p35S:NIGT1.2*, *p35S:NIGT1.4* and *p35S:GFP* in the binary vector pB7WG2) were co-inoculated with pBIN61 P19 (62). Two days after inoculation, leaf discs were punched out and their LUC activities were measured using Dual-Luciferase Reporter Assay System kit (Promega) and SpectraMax M5e (Molecular Devices).

Acknowledgements

We thank N.M. Belliveau and D.W Galbraith for technical advice for FACS, Y. Mizuta for providing research materials, M. Ashikari, H. Tsuji, K. Nagai, and M. Mizutani for scientific discussion. We also thank T. Niwa, A. Furuta, S. Ishikawa and T. Takagi for technical assistance. This research was supported by grants from the National Institutes of Health grant (R01GM079712 to J.T.C., C.Q., and T.I.; NIGMS MIRA grant no. 1R35GM139532 to C.Q.), from the National Science Foundation (PlantSynBio grant no. 2240888 to C.Q), Japan MEXT KAKENHI (JP20H05910 and JP22H04978 to T.I.), JSPS KAKENHI (24K18139 to H.T.) and National Science Foundation grant (NSF-IOS #1755452 to J.L.P.-P.).

Additional information

Data availability

Bulk RNA-seq from sorted nuclei can be found at the NCBI short read archive bio project PRJNA1098062. snRNA-seq can be found at NCBI GEO under GSE273032. The RNA-seq data of *pSUC2:NIGT1.2* and *pSUC2:NIGT1.4* plants have been deposited in the DNA Data Bank of Japan (DDBJ) Sequence Read Archive under PRJDB17784.

Author Contributions

H.T. and T.I conceptualized the study.

Methodology: H.T. and C.M.A.

Investigation: H.T., S.I, J.S.S, A.K., A.K.H., N.L., T.S., J.W., C.Y., C.T.N., J.L.P-P and T.I.

Formal analysis: H.T., T.S., K.L.B., J.L.P.-P. and J.T.C. Data curation: H.T. T.S. and J.T.C.

Validation: H.T., A.K.H., and T.I. Visualization: H.T.

Funding acquisition: H.T., J.L.P.-P., J.T.C., C.Q. and T.I.

Resources: S.I., D.K., T.K. and J.L.P.-P.

Project administration: H.T., C.Q. and T.I.

Supervision: Y.S., Y.T., J.L.P.-P., C.Q. and T.I.

H.T., S.I, J.S., A.K.H, J.T.C., and C.Q. and T.I.

wrote the manuscript. N.L. reviewed and commented on the manuscript.

Funding

National Institutes of Health (R01GM079712)

National Institute of General Medical Sciences (1R35GM139532)

National Science Foundation (PlantSynBio 2240888)

Japan MEXT KAKENHI (JP20H05910)

Japan MEXT KAKENHI (JP22H04978)

JSPS KAKENHI (24K18139)

National Science Foundation (NSF-IOS #1755452)

Additional files

Supplemental information

Supplemental data 1

Supplemental data 2

Supplemental data 3

Supplemental data 4

Supplemental data 5

Supplemental data 6

Supplemental data 7

Supplemental data 8

Supplemental data 9

Supplemental data 10

Supplemental data 11

Supplemental data 12

Supplemental data 13

References

1. Andres F., Coupland G. (2012) **The genetic basis of flowering responses to seasonal cues** *Nat Rev Genet* **13**:627–639 Google Scholar

2. Song Y. H., Shim J. S., Kinmonth-Schultz H. A., Imaizumi T. (2015) **Photoperiodic flowering: time measurement mechanisms in leaves** *Annu Rev Plant Biol* **66**:441–464 Google Scholar

3. Zhu Y., Klasfeld S., Wagner D. (2021) **Molecular regulation of plant developmental transitions and plant architecture via PEPB family proteins: an update on mechanism of action** *J Exp Bot* **72**:2301–2311 Google Scholar

4. Freytes S. N., Canelo M., Cerdán P. D. (2021) **Regulation of Flowering Time: When and Where?** *Curr Opin Plant Biol* **63** Google Scholar

5. Pandey S. P., Benstein R. M., Wang Y., Schmid M. (2021) **Epigenetic Regulation of Temperature Responses - Past Successes and Future Challenges** *J Exp Bot* **72**:7482–7497 Google Scholar

6. Takagi H., Hempton A. K., Imaizumi T. (2023) **Photoperiodic flowering in Arabidopsis: Multilayered regulatory mechanisms of CONSTANS and the florigen FLOWERING LOCUS T** *Plant Commun* **4** Google Scholar

7. Corbesier L., et al. (2007) **FT protein movement contributes to long-distance signaling in floral induction of Arabidopsis** *Science* **316**:1030–1033 Google Scholar

8. Tamaki S., Matsuo S., Wong H. L., Yokoi S., Shimamoto K. (2007) **Hd3a protein is a mobile flowering signal in rice** *Science* **316**:1033–1036 Google Scholar

9. Mathieu J., Warthmann N., Küttner F., Schmid M. (2007) **Export of FT protein from phloem companion cells is sufficient for floral induction in Arabidopsis** *Curr Biol* **17**:1055–1060 Google Scholar

10. Notaguchi M., et al. (2008) **Long-distance, graft-transmissible action of Arabidopsis FLOWERING LOCUS T protein to promote flowering** *Plant Cell Physiol* **49**:1645–1658 Google Scholar

11. Takada S., Goto K. (2003) **TERMINAL FLOWER2, an Arabidopsis homolog of HETEROCHROMATIN PROTEIN1, counteracts the activation of FLOWERING LOCUS T by CONSTANS in the vascular tissues of leaves to regulate flowering time** *Plant Cell* **15**:2856–2865 Google Scholar

12. Chen Q., et al. (2018) **FLOWERING LOCUS T mRNA is synthesized in specialized companion cells in Arabidopsis and Maryland Mammoth tobacco leaf veins** *Proc. Natl. Acad. Sci. U.S.A* **115**:2830–2835 Google Scholar

13. Song Y. H., et al. (2018) **Molecular basis of flowering under natural long-day conditions in Arabidopsis** *Nat. Plants* **4**:824–835 Google Scholar

14. Lee N., et al. (2023) **The FLOWERING LOCUS T gene expression is controlled by high-irradiance response and external coincidence mechanism in long days in Arabidopsis** *New Phytol* **239**:208–221 Google Scholar

15. Takagi H., et al. (2025) **Florigen-producing cells express FPF1-LIKE PROTEIN 1 to accelerate flowering and stem growth in Arabidopsis** *Dev Cell* **60**:1822–1837 Google Scholar

16. Kim J. Y., et al. (2021) **Distinct identities of leaf phloem cells revealed by single cell transcriptomics** *Plant Cell* **33**:511–530 Google Scholar

17. Deal R. B., Henikoff S. (2011) **The INTACT method for cell type-specific gene expression and chromatin profiling in Arabidopsis thaliana** *Nat. Protoc* **6**:56–68 Google Scholar

18. Shi D., et al. (2021) **Tissue-specific transcriptome profiling of the Arabidopsis inflorescence stem reveals local cellular signatures** *Plant Cell* **33**:200–223 Google Scholar

19. Ito S., et al. (2012) **FLOWERING BHLH transcriptional activators control expression of the photoperiodic flowering regulator CONSTANS in Arabidopsis** *Proc Natl Acad Sci U S A* **109**:3582–3587 Google Scholar

20. Zhou Y., et al. (2019) **Metascape provides a biologist-oriented resource for the analysis of systems-level datasets** *Nat. Commun* **10** Google Scholar

21. McInnes L., Healy J., Melville J. (2018) **UMAP: Uniform manifold approximation and projection for dimension reduction** *arXiv* https://doi.org/10.48550/arXiv.1802.03426 | Google Scholar

22. Hunt H., et al. (2023) **Analysis of companion cell and phloem metabolism using a transcriptome-guided model of Arabidopsis metabolism** *Plant Physiol* **192**:1359–1377 Google Scholar

23. Kushwah S., et al. (2020) **Arabidopsis XTH4 and XTH9 contribute to wood cell expansion and secondary wall formation** *Plant Physiol* **182**:1946–1965 Google Scholar

24. Litholdo C. G., et al (2016) **Proteomic identification of putative MicroRNA394 target genes in Arabidopsis thaliana identifies major latex protein family members critical for normal development** *Mol Cell Proteomics* **15**:2033–2047 Google Scholar

25. Wang H., et al. (2016) **Regulatory function of Arabidopsis lipid transfer protein 1 (LTP1) in ethylene response and signaling** *Plant Mol Biol* **91**:471–484 Google Scholar

26. Prado K., et al. (2013) **Regulation of Arabidopsis leaf hydraulics involves light-dependent phosphorylation of aquaporins in veins** *Plant Cell* **25**:1029–1039 Google Scholar

27. Chauvin A., Lenglet A., Wolfender J. L., Farmer E. E. (2016) **Paired hierarchical organization of 13-lipoxygenases in Arabidopsis** *Plants* **5** Google Scholar

28. Kienow L., et al. (2008) **Jasmonates meet fatty acids: functional analysis of a new acyl-coenzyme A synthetase family from Arabidopsis thaliana** *J Exp Bot* **59**:403–419 Google Scholar

29. Li S., Ma J., Liu P. (2013) **OPR3 is expressed in phloem cells and is vital for lateral root development in Arabidopsis** *Canadian Journal of Plant Science* **93**:165–170 Google Scholar

30. Aubry S., Smith-Unna R. D., Boursnell C. M., Kopriva S., Hibberd J. M. (2014) **Transcript residency on ribosomes reveals a key role for the Arabidopsis thaliana bundle sheath in sulfur and glucosinolate metabolism** *Plant J* **78**:659–673 Google Scholar

31. Torii K., et al. (2022) **A guiding role of the Arabidopsis circadian clock in cell differentiation revealed by time-series single-cell RNA sequencing** *Cell Reports* **40** Google Scholar

32. Biedron M., Banasiak A. (2018) **Auxin-mediated regulation of vascular patterning in Arabidopsis thaliana leaves** *Plant Cell Rep* **37**:1215–1229 Google Scholar

33. Yang Y., Costa A., Leonhardt N., Siegel R. S., Schroeder J. I. (2008) **Isolation of a strong Arabidopsis guard cell promoter and its potential as a research tool** *Plant Methods* **4** Google Scholar

34. Jones D. C., et al. (2016) **A clade-specific Arabidopsis gene connects primary metabolism and senescence** *Front Plant Sci* **7** Google Scholar

35. Baxter C. E., Costa M. M., Coen E. S. (2007) **Diversification and co-option of RAD-like genes in the evolution of floral asymmetry** *Plant J* **52**:105–113 Google Scholar

36. Ryu J. Y., et al. (2014) **The Arabidopsis floral repressor BFT delays flowering by competing with FT for FD binding under high salinity** *Mol Plant* **7**:377–387 Google Scholar

37. Dreos R., Ambrosini G., Perier R. C., Bucher P. (2015) **The Eukaryotic Promoter Database: expansion of EPDnew and new promoter analysis tools** *Nucleic Acids Res* **43**:D92–96 Google Scholar

38. Meylan P., Dreos R., Ambrosini G., Groux R., Bucher P., in EPD (2020) **enhanced data visualization and extension to ncRNA promoters** *Nucleic Acids Res* **48**:D65–D69 Google Scholar

39. Kiba T., et al. (2018) **Repression of nitrogen starvation responses by members of the Arabidopsis GARP-type transcription factor NIGT1/HRS1 subfamily** *Plant Cell* **30**:925–945 Google Scholar

40. Maeda Y., et al. (2018) **A NIGT1-centred transcriptional cascade regulates nitrate signalling and incorporates phosphorus starvation signals in Arabidopsis** *Nat Commun* **9** Google Scholar

41. Adrian J., et al. (2010) **, cis-Regulatory elements and chromatin state coordinately control temporal and spatial expression of FLOWERING LOCUS T in Arabidopsis** *Plant Cell* **22**:1425–1440 Google Scholar

42. Tiwari S. B., et al. (2010) **The flowering time regulator CONSTANS is recruited to the FLOWERING LOCUS T promoter via a unique cis-element** *New Phytol* **187**:57–66 Google Scholar

43. Bonaldi K., Li Z., Kang S. E., Breton G., Pruneda-Paz J. L. (2017) **Novel cell surface luciferase reporter for high-throughput yeast one-hybrid screens** *Nucleic Acids Res* **45**:e157 Google Scholar

44. Li Z., Bonaldi K., Kang S. E., Pruneda-Paz J. L. (2019) **High-Throughput Yeast One-Hybrid Screens Using a Cell Surface gLUC Reporter** *Curr Protoc Plant Biol* **4**:e20086 Google Scholar

45. Sanagi M., et al. (2021) **Low nitrogen conditions accelerate flowering by modulating the phosphorylation state of FLOWERING BHLH 4 in Arabidopsis** *Proc Natl Acad Sci U S A* **118**:e2022942118 Google Scholar

46. Yoo S. J., et al. (2010) **BROTHER OF FT AND TFL1 (BFT) has TFL1-like activity and functions redundantly with TFL1 in inflorescence meristem development in Arabidopsis** *Plant J* **63**:241–253 Google Scholar

47. Higuchi Y. (2018) **Florigen and anti-florigen: flowering regulation in horticultural crops** *Breed Sci* **68**:109–118 Google Scholar

48. Higuchi Y., et al. (2013) **The gated induction system of a systemic floral inhibitor, antiflorigen, determines obligate short-day flowering in chrysanthemums** *Proc Natl Acad Sci U S A* **110**:17137–17142 Google Scholar

49. Soyk S., et al. (2017) **Variation in the flowering gene SELF PRUNING 5G promotes day-neutrality and early yield in tomato** *Nat Genet* **49**:162–168 Google Scholar

50. Zhu Y., et al. (2020) **TERMINAL FLOWER 1-FD complex target genes and competition with FLOWERING LOCUS T** *Nat Commun* **11** Google Scholar

51. McKim S. M. (2020) **Moving on up - controlling internode growth** *New Phytol* **226**:672–678 Google Scholar

52. Maxwell B. B., Andersson C. R., Poole D. S., Kay S. A., Chory J. (2003) **HY5, Circadian Clock-Associated 1, and a cis-element, DET1 dark response element, mediate DET1 regulation of chlorophyll a/b-binding protein 2 expression** *Plant Physiol* **133**:1565–1577 Google Scholar

53. Nakagawa T., et al. (2008) **Development of R4 gateway binary vectors (R4pGWB) enabling high-throughput promoter swapping for plant research** *Biosci Biotechnol Biochem* **72**:624–629 Google Scholar

54. Galbraith D. W. (2014) **Flow Cytometry and Sorting in Arabidopsis** In: Sanchez-Serrano J., Salinas J., editors. *Arabidopsis Protocols, 3rd Edition* Springer pp. 509–537 https://doi.org/10.1007/978-1-62703-580-4_27 | Google Scholar

55. Dobin A., et al. (2013) **STAR: ultrafast universal RNA-seq aligner** *Bioinformatics* **29**:15–21 Google Scholar

56. Hao Y., et al. (2021) **Integrated analysis of multimodal single-cell data** *Cell* **184**:3573–3587 Google Scholar

57. Satija R., Farrell J. A., Gennert D., Schier A. F., Regev A. (2015) **Spatial reconstruction of single-cell gene expression data** *Nat Biotechnol* **33**:495–502 Google Scholar

58. Bailey T. L., Grant C. E. (2021) **SEA: Simple Enrichment Analysis of motifs** *bioRxiv* https://doi.org/10.1101/2021.08.23.457422 | Google Scholar

59. Suzuki T., et al. (2022) **The DROL1 subunit of U5 snRNP in the spliceosome is specifically required to splice AT-AC-type introns in Arabidopsis** *Plant J* **109**:633–648 Google Scholar

60. Schultz T. F., Kiyosue T., Yanovsky M., Wada M., Kay S. A. (2001) **A role for LKP2 in the circadian clock of Arabidopsis** *Plant Cell* **13**:2659–2670 Google Scholar

61. Kubota A., et al. (2017) **TCP4-dependent induction of CONSTANS transcription requires GIGANTEA in photoperiodic flowering in Arabidopsis** *PLoS Genet* **13**:e1006856 Google Scholar

62. Voinnet O., Rivas S., Mestre P., Baulcombe D. (2003) **An enhanced transient expression system in plants based on suppression of gene silencing by the p19 protein of tomato bushy stunt virus** *Plant J* **33**:949–956 Google Scholar

Author information

Hiroshi Takagi
Department of Biology, University of Washington, Seattle, United States, Center for Gene Research, Nagoya University, Nagoya, Japan, Bioscience and Biotechnology Center, Nagoya University, Nagoya, Japan, Institute for Advanced Research (IAR), Nagoya University, Nagoya, Japan
ORCID iD: 0000-0003-0321-0284

Shogo Ito
Department of Biology, University of Washington, Seattle, United States, Department of Botany, Graduate School of Science, Kyoto University, Kyoto, Japan
ORCID iD: 0000-0002-8434-6652

Jae Sung Shim
Department of Biology, University of Washington, Seattle, United States, School of Biological Sciences and Technology, Chonnam National University, Gwangju, Republic of Korea
ORCID iD: 0000-0002-7352-437X

Akane Kubota
Department of Biology, University of Washington, Seattle, United States, Division of Biological Science, Nara Institute of Science and Technology, Nara, Japan
ORCID iD: 0000-0003-1347-3950

Andrew K Hempton
Department of Biology, University of Washington, Seattle, United States
ORCID iD: 0000-0002-3018-6091

Nayoung Lee
Department of Biology, University of Washington, Seattle, United States, Research Institute of Molecular Alchemy (RIMA), Gyeongsang National University, Jinju, Republic of Korea
ORCID iD: 0000-0002-0353-6455

Takamasa Suzuki
Department of Biological Chemistry, College of Bioscience and Biotechnology, Chubu University, Kasugai, Japan

ORCID iD: 0000-0002-1977-0510

Jared S Wong
Department of Biology, University of Washington, Seattle, United States

Chansie Yang
Department of Biology, University of Washington, Seattle, United States
ORCID iD: 0000-0002-8118-2883

Christine T Nolan
Department of Biology, University of Washington, Seattle, United States
ORCID iD: 0009-0001-9257-9595

Kerry L Bubb
Department of Genome Sciences, University of Washington, Seattle, United States
ORCID iD: 0000-0002-1117-2591

Cristina M Alexandre
Department of Genome Sciences, University of Washington, Seattle, United States
ORCID iD: 0000-0003-0047-0312

Daisuke Kurihara
Institute for Advanced Research (IAR), Nagoya University, Nagoya, Japan, Institute of Transformative Bio-Molecules (WPI-ITbM), Nagoya University, Nagoya, Japan
ORCID iD: 0000-0003-2703-0405

Yoshikatsu Sato
Institute of Transformative Bio-Molecules (WPI-ITbM), Nagoya University, Nagoya, Japan
ORCID iD: 0000-0002-4967-2698

Yasuomi Tada
Center for Gene Research, Nagoya University, Nagoya, Japan, Division of Biological Science, Graduate School of Science, Nagoya University, Nagoya, Japan
ORCID iD: 0000-0001-9900-069X

Takatoshi Kiba
Graduate School of Bioagricultural Sciences, Nagoya University, Nagoya, Japan, RIKEN Center for Sustainable Resource Science, Yokohama, Japan
ORCID iD: 0000-0001-8651-0404

Jose L Pruneda-Paz
School of Biological Sciences, University of California, San Diego, La Jolla, United States, Center for Circadian Biology, University of California, San Diego, La Jolla, United States
ORCID iD: 0000-0002-0054-0918

Christine Queitsch
Department of Genome Sciences, University of Washington, Seattle, United States, Brotman Baty Institute for Precision Medicine, University of Washington, Seattle, United States
ORCID iD: 0000-0002-0905-4705

Josh T Cuperus
Department of Genome Sciences, University of Washington, Seattle, United States, Brotman Baty Institute for Precision Medicine, University of Washington, Seattle, United States
ORCID iD: 0000-0002-8019-7733

Takato Imaizumi
Department of Biology, University of Washington, Seattle, United States
ORCID iD: 0000-0001-9396-4412

For correspondence: takato@uw.edu

Editors

Reviewing Editor
Pil Joon Seo
Seoul National University, Seoul, Republic of Korea

Senior Editor
Jürgen Kleine-Vehn
University of Freiburg, Freiburg, Germany

Reviewer #1 (Public review):

Summary:

The authors revealed the cellular heterogeneity of companion cells (CCs) and demonstrated that the florigen gene FT is highly expressed in a specific subpopulation of these CCs in Arabidopsis. Through a thorough characterization of this subpopulation, they further identified NITRATE-INDUCIBLE GARP-TYPE TRANSCRIPTIONAL REPRESSOR 1 (NIGT1)-like transcription factors as potential new regulators of FT. Overall, these findings are intriguing and valuable, contributing significantly to our understanding of florigen and the photoperiodic flowering pathway. However, there is still room for improvement in the quality of the data and the depth of the analysis. I have several comments that may be beneficial for the authors.

Strengths:

The usage of snRNA-seq to characterize the FT-expressing companion cells (CCs) is very interesting and important. Two findings are novel: 1) Expression of FT in CCs is not uniform. Only a subcluster of CCs exhibits high expression level of FT. 2) Based on consensus binding motifs enriched in this subcluster, they further identify NITRATE-INDUCIBLE GARP-TYPE TRANSCRIPTIONAL REPRESSOR 1 (NIGT1)-like transcription factors as potential new regulators of FT.

Weaknesses:

(1) Title: "A florigen-expressing subpopulation of companion cells". It is a bit misleading. The conclusion here is that only a subset of companion cells exhibit high expression of FT, but this does not imply that other companion cells do not express it at all.

(2) Data quality: Authors opted for fluorescence-activated nuclei sorting (FANS) instead of traditional cell sorting method. What is the rationale behind this decision? Readers may wonder, especially given that RNA abundance in single nuclei is generally lower than that in single cells. This concern also applies to snRNA-seq data. Specifically, the number of genes

captured was quite low, with a median of only 149 genes per nucleus. Additionally, the total number of nuclei analyzed was limited (1,173 for the pFT:NTF and 3,650 for the pSUC2:NTF). These factors suggest that the quality of the snRNA-seq data presented in this study is quite low. In this context, it becomes challenging for the reviewer to accurately assess whether this will impact the subsequent conclusions of the paper. Would it be possible to repeat this experiment and get more nuclei?

(3) Another disappointment is that the authors did not utilize reporter genes to identify the specific locations of the FT-high expressing cells (cluster 7 cells) within the CC population in vivo. Are there any discernible patterns that can be observed?

(4) The final disappointment is that the authors only compared FT expression between the nigtQ mutants and the wild type. Does this imply that the mutant does not have a flowering time defect particularly under high nitrogen conditions?

Comments on revisions:

I think the authors took my comments seriously and addressed most of my concerns. Overall, I find this to be a very interesting paper.

https://doi.org/10.7554/eLife.102529.2.sa2

Reviewer #2 (Public review):

This manuscript submitted by Takagi et al. details the molecular characterization of the FT-expressing cell at a single-cell level. The authors examined what genes are expressed specifically in FT-expressing cells and other phloem companion cells by exploiting bulk nuclei and single-nuclei RNA-seq and transgenic analysis. The authors found the unique expression profile of FT-expressing cells at a single-cell level and identified new transcriptional repressors of FT such as NIGT1.2 and NIGT1.4.

Although previous researchers have known that FT is expressed in phloem companion cells, they have tended to neglect the molecular characterization of the FT-expressing phloem companion cells. To understand how FT, which is expressed in tiny amounts in phloem companion cells that make up a very small portion of the leaf, can be a key molecule in the regulation of the critical developmental step of floral transition, it is important to understand the molecular features of FT-expressing cells in detail. In this regard, this manuscript provides insight into the understanding of detailed molecular characteristics of the FT-expressing cell. This endeavor will contribute to the research field of flowering time.

During the initial review process, I proposed the following two points for improving this manuscript:

(1) The most noble finding of this manuscript is the identification of NTGI1.2 as the upstream regulator of FT-expressing cluster 7 gene expression. The flowering phenotypes of the nigtQ mutant and the transgenic plants in which NIGT1.2 was expressed under the SUC2 gene promoter support that NIGT1.2 functions as a floral repressor upstream of the FT gene. Nevertheless, the expression patterns of NIGT1.2 genes do not appear to have much overlap with those of NIGT1.2-downstream genes in the cluster 7 (Figs S14 and F3). An explanation for this should be provided in the discussion section.

(2) To investigate gene expression in the nuclei of specific cell populations, the authors generated transgenic plants expressing a fusion gene encoding a Nuclear Targeting Fusion protein (NTF) under the control of various cell type-specific promoters. Since the public audience would not know about NTF without reading reference 16, some explanation of NTF

is necessary in the manuscript. Please provide a schematic of the constructs the authors used to make the transformants.

The revised manuscript has addressed my comments well. I am deeply grateful for the authors' efforts to address concerns raised by me and other reviewers.
I have no doubt that the manuscript in its current form is worthy of publication in this journal and will provide valuable insights into flowering time for many readers.

https://doi.org/10.7554/eLife.102529.2.sa1

Author response:

The following is the authors' response to the original reviews.

> ***Reviewer #1 (Public review):***
>
> *Summary:*
>
> *The authors revealed the cellular heterogeneity of companion cells (CCs) and demonstrated that the florigen gene FT is highly expressed in a specific subpopulation of these CCs in Arabidopsis. Through a thorough characterization of this subpopulation, they further identified NITRATE-INDUCIBLE GARP-TYPE TRANSCRIPTIONAL REPRESSOR 1 (NIGT1)-like transcription factors as potential new regulators of FT. Overall, these findings are intriguing and valuable, contributing significantly to our understanding of florigen and the photoperiodic flowering pathway. However, there is still room for improvement in the quality of the data and the depth of the analysis. I have several comments that may be beneficial for the authors.*
>
> *Strengths:*
>
> *The usage of snRNA-seq to characterize the FT-expressing companion cells (CCs) is very interesting and important. Two findings are novel: 1) Expression of FT in CCs is not uniform. Only a subcluster of CCs exhibits high expression level of FT. 2) Based on consensus binding motifs enriched in this subcluster, they further identify NITRATE-INDUCIBLE GARP-TYPE TRANSCRIPTIONAL REPRESSOR 1 (NIGT1)-like transcription factors as potential new regulators of FT.*

We are pleased to hear that reviewer 1 noted the novelty and importance of our work. As reviewer 1 mentioned, we are also excited about the identification of a subcluster of companion cells with very high FT expression. We believe that this work is an initial step to describe the molecular characteristics of these FT-expressing cells. We are also excited to share our new findings on NIGT1s as potential FT regulators. We believe this finding will attract a broader audience, as the molecular factor coordinating plant nutrition status with flowering time remains largely unknown despite its well-known phenomenon.

> *Weaknesses:*
>
> *(1) Title: "A florigen-expressing subpopulation of companion cells". It is a bit misleading. The conclusion here is that only a subset of companion cells exhibit high expression of FT, but this does not imply that other companion cells do not express it at all.*

We agree with this comment, as it was not our intention to sound like that FT is not produced in other companion cells than the subpopulation we identified. We revised the title to more accurately reflect the point. The new title is "Companion cells with high florigen production express other small proteins and reveal a nitrogen-sensitive FT repressor."

> *(2) Data quality: Authors opted for fluorescence-activated nuclei sorting (FANS) instead of traditional cell sorting method. What is the rationale behind this decision? Readers may wonder, especially given that RNA abundance in single nuclei is generally lower than that in single cells. This concern also applies to snRNA-seq data. Specifically, the number of genes captured was quite low, with a median of only 149 genes per nucleus. Additionally, the total number of nuclei analyzed was limited (1,173 for the pFT:NTF and 3,650 for the pSUC2:NTF). These factors suggest that the quality of the snRNA-seq data presented in this study is quite low. In this context, it becomes challenging for the reviewer to accurately assess whether this will impact the subsequent conclusions of the paper. Would it be possible to repeat this experiment and get more nuclei?*

We appreciate this comment; we noticed that we did not clearly explain the rationale for using single-nucleus RNA sequencing (snRNA-seq) instead of single-cell RNA-seq (scRNA-seq). As reviewer 1 mentioned, RNA abundance in scRNA-seq is higher than in snRNA-seq. To conduct scRNA-seq using plant cells, protoplasting is the necessary step. However, in our study, protoplasting has many drawbacks in isolating our target cells from the phloem. First, it is technically challenging to efficiently isolate protoplasts from highly embedded phloem companion cells from plant tissues. Typically, at least several hours of enzymatic incubation are required to obtain protoplasts from companion cells (often using semi-isolated vasculatures), and the efficiency of protoplasting vasculature cells remains low. Secondly, for our analysis, restoring the time information within a day is also crucial. Therefore, we employed a more rapid isolation method. In the revision, we will explain our rationale for choosing snRNA-seq due to the technical limitations. In the revised manuscripts, we added four new sentences in the Introduction section to clearly explain these points.

Reviewer 1 also raised a concern about the quality of our snRNA-seq data, referring to the relatively low readcounts per nucleus. Although we believe that shallow reads do not necessarily indicate low quality and are confident in the accuracy of our snRNA-seq data, as supported by the detailed follow-up experiments (e.g., imaging analysis in Fig. 4B), we agree that it is important to address this point in the revision and alleviate readers' concerns regarding the data quality.

We believe the primary reason for the low readcounts per cell is the small amount of RNA present in each Arabidopsis vascular cell nucleus that we isolated. For bulk nuclei RNAseq, we collected 15,000 nuclei. However, the total RNA amount was approximately 3 ng. It indicates that each nucleus isolated contains a very limited amount of RNA (by the simple calculation, 3,000 pg / 15,000 nuclei = 0.2 pg/nucleus). It appears that the size of cells and nuclei was still small in 2-week-old seedlings; thus, each nucleus may contain lower levels of RNA. During the optimization process, we also tried to fix the tissues that we hoped to restore nuclear retained RNA, but unfortunately, in our hands, we encountered the technical issue of nuclei aggregation that hindered the sorting process, which is not suitable for single-nucleus RNA-seq.

Reviewer 1 suggested that we repeat the same snRNA-seq experiment. We agree that having more cells increases the reliability of data. However, to our knowledge, higher cell numbers enhance the confidence of clustering, but not readcounts per cell. In our snRNAseq data, our target, FT-expressing cells, were observed in cluster 7, which projected at an obvious distance from other cell clusters. Therefore, we think that having more nuclei does not significantly help in separating high FT-expressing cluster 7 cells and different types of cells, although we may obtain more DEGs from the cluster 7 cells. Considering the costs and time required for additional snRNA-seq experiments, we think that adding more followup molecular biology experiment data would be more practical. We clearly stated the limitations of our approach in the Discussion section. "A drawback of our snRNA-seq analysis was shallow reads per nucleus. It appears mainly due to the low abundance of mRNA in nuclei from 2-week-old

leaves. Based on our calculation, the average mRNA level per nucleus is approximately 0.2 pg (3,000 pg mRNA from 15,000 sorted nuclei). Future technological advance is needed to improve the data quality“

In this revised version of the manuscript, we silenced FT gene expression using an amiRNA against FT driven by tissue-specific promoters [pROXY10, cluster 7; pSUC2, companion cells; pPIP2.6, cluster 4 (for the spatial expression pattern of PIP2.6, please see the new data shown in Fig. S8F); pGC1, guard cells]. Given that both FT and ROXY10 were highly expressed in cluster 7 of our snRNA-seq dataset, we anticipated the late flowering phenotype of pROXY10:amiRNA-ft. As we expected, pROXY10:amiR-ft but not pPIP2.6:amiR-ft lines showed delayed flowering phenotypes (Fig. S14A), supporting the validity of our snRNA-seq approach. We are also now more confident in the resolution of our snRNA-seq analysis, since cluster 4-specific PIP2.6 did not cause late flowering despite its higher basal expression than ROXY10 (Fig. S14B).

> *(3) Another disappointment is that the authors did not utilize reporter genes to identify the specific locations of the FT-high expressing cells (cluster 7 cells) within the CC population in vivo. Are there any discernible patterns that can be observed?*

In the original manuscript, as we showed only limited spatial images of overlap between FT and other cluster 7 genes in Fig. 4B, this comment is totally understandable. To respond to it, we added whole leaf images showing the spatial expression of FT and other cluster 7 genes (Fig. S12). These data indicate that cluster 7 genes including FT are expressed highly in minor veins in the distal part of the leaf but weakly in the main vein. We also added enlarged images of spatial expression of FT and cluster 7 genes (FLP1 and ROXY10) to note that those genes do not overlap completely (Fig. S13).

In contrast to cluster 7 genes, genes highly expressed in cluster 4, such as LTP1 and MLP28, are reportedly highly expressed in the main leaf vein. To further confirm it, we established a transgenic line that expresses a GFP-fusion protein controlled by the promoter of a cluster 4-specific gene PIP2.6 (Fig. S8F). It also showed strong GFP signals in the main vein, consistent with previous observations of LTP1 and MLP28. In summary, FT-expressing cells (cluster 7 cells) are enriched in companion cells in the minor vein, and their expression patterns show a clear distinction from genes expressed in the main vein (e.g., cluster 4-specific genes).

> *(4) The final disappointment is that the authors only compared FT expression between the nigtQ mutants and the wild type. Does this imply that the mutant does not have a flowering time defect particularly under high nitrogen conditions?*

We agree with reviewer 1 that more experiments are required to conclude the role of NIGT1 on FT regulation, in addition to our Y1H data, flowering time data of NIGT1 overexpressors, and FT expression in NIGT1 overexpressors and nigtQ mutant.

First, to test the direct regulation of NIGT1s on FT transcription, we conducted a transient luciferase (LUC) assay in tobacco leaves using effectors (p35S:NIGT1.2, p35S:NIGT1.4, and p35S:GFP) and reporters [pFT:LUC (FT promoter fused with LUC) and pFTm:LUC (the same FT promoter with mutations in NIGT1-binding sites fused with LUC)]. Our result showed that NIGT1.2 and NIGT1.4, but not GFP, decreased the activity of pFT:LUC but not pFTm:LUC (Fig. 5C). This indicates that NIGT1s directly repress the FT gene.

Second, to address reviewer 1’s suggestion about the effect of of nigtQ mutation on flowering time, we have grown WT and nigtQ plants on 20 mM and 2 mM NH_4NO_3. Under 20 mM NH_4NO_3, the nigtQ line bolted at earlier days than WT; under 2 mM NH_4NO_3, nigtQ and WT bolted at almost same timing (Fig. S17D and E). This result suggests that the nigtQ mutation affects flowering timing depending on nitrogen nutrient status. However, leaf numbers of

bolted plants were not different between WT and nigtQ lines (Fig. S17E). Therefore, it appears that nigtQ mutation also accelerated overall growth of plants rather than flowering promotion. We also have measured flowering time by counting leaf numbers of the nigtQ and WT plants at bolting on nitrogen-rich soil. The mutant generated slightly more leaves than WT when they flowered (Fig. S17G). These results suggest that the NIGT-derived fine-tuning of FT regulation is conditional on higher nitrogen conditions.

> *Minor:*
>
> *(1) Abstract: "Our bulk nuclei RNA-seq demonstrated that FT-expressing cells in cotyledons and in true leaves differed transcriptionally.". This sentence is not informative. What exactly is the difference in FT-expressing cells between cotyledons and true leaves?*

We modified the sentence to clarify the differences between cotyledons and true leaves. “Our bulk nuclei RNA-seq demonstrated that FT-expressing cells in cotyledons and true leaves showed differences especially in FT repressor genes.”

> *(2) As a standard practice, to support the direct regulation of FT by NIGT1, the authors should provide EMSA and ChIP-seq data. Ideally, they should also generate promoter constructs with deletions or mutations in the NIGT1 binding sites.*

To test direct interaction of NIGT1 to the FT promoter sequences, we performed the transient reporter assay using FT promoter driven luciferase reporter (Fig. 5C). NIGT1.2 and NIGT1.4 repressed the FT promoter activity; however, with NIGT1 binding site mutations, this repression was not observed, indicating that NIGT1 binds to the ciselements in the FT promoter to repress its transcription.

> *(3) Sorting: Did the authors fix the samples before preparing the nuclei suspension? If not, could this be the reason the authors observed the JA-responsive clusters (Fig. 2J)? Please provide more details related to nuclei sorting in the Methods section.*

We added a new subsection in the Materials and Methods section to explain a detail of the nuclei sorting procedure. We did not include a sample fixation step. We have tried formaldehyde fixation; however, it clumped nuclei, which was not suitable for snRNA-seq. Moreover, fixation steps generally reduce readcounts of single-cell RNA-seq according to the 10X Genomics’ guideline.

We agree that JA responses were triggered during the FANS nuclei isolation. Therefore, we added the following sentence. “Since our FANS protocol did not include a sample fixation step to avoid clumping, these cells likely triggered wounding responses during the chopping and sorting process (Fig. S1B).

> ***Reviewer #2 (Public review):***
>
> *This manuscript submitted by Takagi et al. details the molecular characterization of the FTexpressing cell at a single-cell level. The authors examined what genes are expressed specifically in FT-expressing cells and other phloem companion cells by exploiting bulk nuclei and single-nuclei RNA-seq and transgenic analysis. The authors found the unique expression profile of FT-expressing cells at a single-cell level and identified new transcriptional repressors of FT such as NIGT1.2 and NIGT1.4.*
>
> *Although previous researchers have known that FT is expressed in phloem companion cells, they have tended to neglect the molecular characterization of the FT-expressing phloem companion cells. To understand how FT, which is expressed in tiny amounts in phloem companion cells that make up a very small portion of the leaf, can be a key*

> *molecule in the regulation of the critical developmental step of floral transition, it is important to understand the molecular features of FT-expressing cells in detail. In this regard, this manuscript provides insight into the understanding of detailed molecular characteristics of the FT-expressing cell. This endeavor will contribute to the research field of flowering time.*
>
> *We are grateful that reviewer 2 recognizes the importance of transcriptome profiling of FTexpressing cells at the single-cell level.*
>
> *Here are my comments on how to improve this manuscript.*
>
> *(1) The most noble finding of this manuscript is the identification of NTGI1.2 as the upstream regulator of FT-expressing cluster 7 gene expression. The flowering phenotypes of the nigtQ mutant and the transgenic plants in which NIGT1.2 was expressed under the SUC2 gene promoter support that NIGT1.2 functions as a floral repressor upstream of the FT gene. Nevertheless, the expression patterns of NIGT1.2 genes do not appear to have much overlap with those of NIGT1.2-downstream genes in the cluster 7 (Figs S14 and F3). An explanation for this should be provided in the discussion section.*

We agree with reviewer 2 that the spatial expression patterns of NIGT1.2 and cluster 7 genes do not overlap much, and some discussion should be provided in the manuscript. Although we do not have a concrete answer for this phenomenon, we obtained the new data showing that NIGT1.2 and NIGT1.4 directly repress the FT gene in planta (Fig. 5C). As NIGT1.2/1.4 are negative regulators of FT, it is plausible that NIGT1.2/1.4 may suppress FT gene expression in non-cluster 7 cells to prevent the misexpression of FT. We added this point in the Results section.

> *(2) To investigate gene expression in the nuclei of specific cell populations, the authors generated transgenic plants expressing a fusion gene encoding a Nuclear Targeting Fusion protein (NTF) under the control of various cell type-specific promoters. Since the public audience would not know about NTF without reading reference 16, some explanation of NTF is necessary in the manuscript. Please provide a schematic of constructs the authors used to make the transformants.*

As reviewer 2 pointed out, we lacked a clear explanation of why we used NTF in this study. NTF is the fusion protein that consists of a nuclear envelope targeting WPP domain, GFP, and a biotin acceptor peptide. It was initially designed for the INTACT (isolation of nuclei tagged in specific cell types) method, which enables us to isolate bulk nuclei from specific tissues. Although our original intention was to profile the bulk transcriptome of mRNAs that exist in nuclei of the FT-expressing cells using INTACT, we utilized our NTF transgenic lines for snRNA-seq analysis. To explain what NTF is to readers, we included a schematic diagram of NTF (Fig. S1A) and more explanation about NTF in the Results section.

Again, we appreciate all reviewers' careful and constructive comments. With these changes, we hope our revised manuscript is now satisfactory.

https://doi.org/10.7554/eLife.102529.2.sa0